Table III—Mean Urinary Recovery and Renal Clearance (±*SD*) of Indomethacin Following Single Doses in Six Subjects

Treatment	Renal Clearance, ml/min	Percent Recovered in Urine
Capsules	32.4 ± 14.3	17.3 ± 12.5
EOP-7/85	33.9 ± 11.9	22.3 ± 7.7
EOP-9/85	35.1 ± 11.4	23.8 ± 5.9
EOP-12/85	42.1 ± 14.2	28.1 ± 7.1

The average zero-order rate for systems that delivered for a time period ≤6 hr was found to be:

In vitro:

$$\bar{Z}_1 = \frac{\sum_i^{12} Z_i}{12} = 10.8 \pm 9.4\% \qquad \text{(Eq. 8)}$$

In vivo:

$$\bar{Z}_2 = \frac{\sum_i^{12} Z_i}{12} = 10.6 \pm 16\% \qquad \text{(Eq. 9)}$$

The *in vitro* and *in vivo* rates are equal and are not significantly different from the rate obtained by the differential method.

Plasma Concentrations and Extent of Drug Absorption from Two Limited Studies in Humans—Plasma profiles from the single-dose study illustrated the controlled-release properties of the EOP-indomethacin dosage forms. Compared with the indomethacin capsules, they produced more constant and prolonged plasma levels (Fig. 11); renal clearance and total urinary recoveries of indomethacin and conjugates are shown in Table III. Relative to capsules of indomethacin, which are known to be completely absorbed (5, 7), the bioavailability of the 7/85, 9/85, and 12/85 systems were estimated to be 0.80, 0.84, and 0.88, respectively (10, 11).

Total 120-hr urinary recovery of indomethacin (free and conjugated) for the multiple-dose study was 130.2 ± 26.7, 139.4 ± 8.9, and 147.7 ± 23.1 mg, respectively, following EOP-indomethacin 7/85, 9/85, and 12/85, and was 128.8 ± 39.1 mg following indomethacin capsules. Similar urinary recovery of indomethacin suggests comparable bioavailability.

Summary—Preliminary studies in humans showed that the extent of absorption from EOP-indomethacin systems 7/85, 9/85, and 12/85 is similar to that after 75 mg of indomethacin in capsules. Plasma concentration profiles are consistent with the planned differences in drug delivery rate and the anticipated effects of enterohepatic circulation (5–7).

REFERENCES

(1) S. E. DeJongh and M. Wijnans, *Acta Physiol. Pharmacol. Neerlandica*, **1**, 237 (1950).

(2) A. G. M. Van Gemert and J W. Duyff, *ibid.*, **1**, 256 (1950).

(3) A. C. Wood, G. A. Glaubiger, and T. N. Chase, *Lancet*, **i**, 1391 (1973).

(4) F. Theeuwes, *J. Pharm. Sci.*, **64**, 1987 (1975).

(5) K. C. Kwan, G. O. Breault, E. R. Umbenhauer, F. G. McMahon, and D. E. Duggan, *J. Pharmacokinet. Biopharm.*, **4**, 225 (1976).

(6) J. Alvan, M. Orme, L. Bertilsson, R. Ekstrand, and L. Palmer, *Clin. Pharmacol. Ther.*, **18**, 364 (1975).

(7) K. C. Kwan, G. O. Breault, R. L. Davis, B. W. Lei, A. W. Czerwinski, G. H. Besselaar, and D. E. Duggan, *J. Pharmacokinet. Biopharm.*, **6**, 451 (1978).

(8) P. Bonsen, P. S. Wong, F. Theeuwes, U.S. Pat. 4,265,874 (1981).

(9) W. F. Bayne, T. East, and D. Dye, *J. Pharm. Sci.*, **70**, 458 (1981).

(10) K. C. Kwan and A. E. Till, *ibid.*, **62**, 1499 (1973).

(11) S. Hwang and K. C. Kwan, *ibid.*, **69**, 77 (1980).

Prediction of Stability in Pharmaceutical Preparations XX: Stability Evaluation and Bioanalysis of Cocaine and Benzoylecgonine by High-Performance Liquid Chromatography

EDWARD R. GARRETT ˣ and KAZIMIERZ SEYDA

Received December 7, 1981 from *The Beehive, College of Pharmacy, J. Hillis Miller Health Center, University of Florida, Gainesville, FL 32610.* Accepted for publication April 22, 1982.

Abstract □ Specific, sensitive, reverse-phase high-performance liquid chromatographic (HPLC) assays of cocaine (I) and its hydrolysis products, benzoylecgonine (II) and benzoic acid (III), have been devised with analytical sensitivities as low as 15 ng/ml of plasma for I using spectrophotometric detection at 232 nm. Cocaine can be separated from its hydrolysis products by extraction at pH 7.5 with haloalkanes. Benzoylecgonine and benzoic acid can be extracted at pH 3.0 with 1-butanol. The evaporated residues were reconstituted in acetonitrile–water for HPLC assay. The assay was used to determine the stabilities of I and II in aqueous solutions, to establish log k–pH profiles at various temperatures, and to evaluate Arrhenius' parameters. Hydrolyses were by specific acid–base catalysis. Cocaine showed hydrogen and hydroxyl ion attack on protonated I with 40 and 90% proceeding through the benzoylecgonine route, respectively, as well as hydroxyl ion attack on neutral cocaine, with only 6% proceeding through the benzoylecgonine route. Cocaine is relatively unstable in the neutral pH range with a half-life of 5 hr in buffer at pH 7.25 and 40°. Similar half-lives were observed in fresh dog plasma at 300 and 30 μg/ml, although one study at 0.5 μg/ml indicated a doubling of the rate.

Keyphrases □ Cocaine—stability evaluation and bioanalysis, hydrolysis products, high-performance liquid chromatography □ High-performance liquid chromatography—cocaine, benzoylecgonine, and benzoic acid in buffers in biological fluids □ Stability—prediction and bioanalysis of cocaine and benzoylecgonine in plasma and buffers, high-performance liquid chromatography □ Benzoylecgonine—hydrolysis product of cocaine, stability evaluation and bioanalysis by high-performance liquid chromatography □ Protein binding—cocaine and its hydrolysis products, benzoylecgonine and benzoic acid, stability evaluation and bioanalysis, high-performance liquid chromatography

Cocaine (I) is metabolized *in vivo*, principally to its solvolytic products (1, 2), with an apparent terminal half-life in humans ranging between 40 and 91 min (3). Although available data on the stability of I in plasma *in vitro* is sparse (3), a rough estimate of the half-life in human plasma of 150 min at 25° can be made.

0022-3549/83/0300-0258$01.00/0

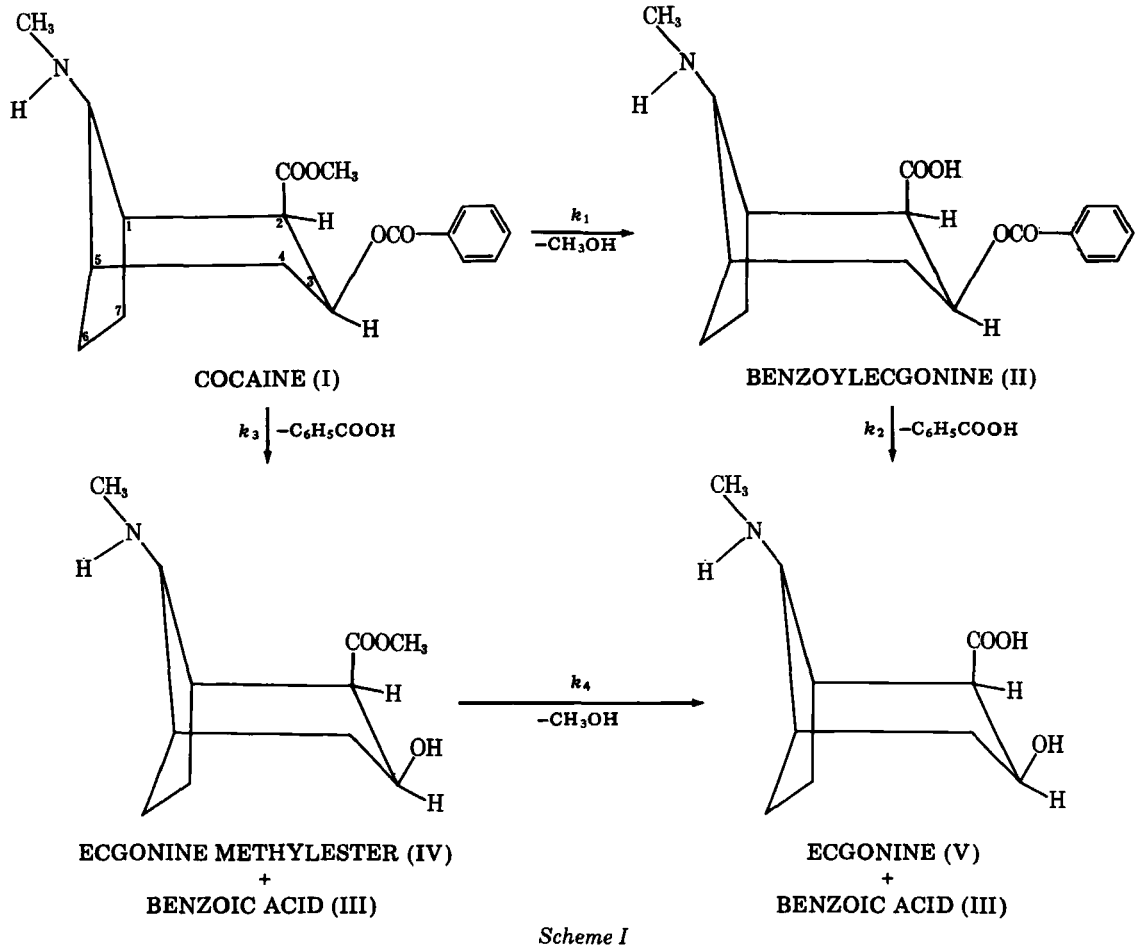

Scheme I

The aqueous solvolysis of 10 mg of I/ml was studied by assaying unchanged drug with time between pH 1 and 8.8 (5). Cocaine was extracted with ether from 5% sodium bicarbonate solutions and spectrophotometrically assayed after reextraction into 0.01 *N* HCl. The maximum stability was stated to be at pH 1.95 and benzoylecgonine (II) was claimed to be the solvolytic product (5).

The present study develops and applies specific and sensitive HPLC assays of I and its solvolytic products (Scheme I) to kinetic studies of stability and mechanisms of solvolyses of both I and II in aqueous and biological fluids, and establishes complete log k–pH profiles at several temperatures in preparation of systematic pharmacokinetic investigations of the drug and its metabolites. The validity of the use of basic physicochemical relations in predicting the stability of drugs under all conditions and optimizing valid assays has been demonstrated (6–9).

An HPLC assay has been claimed to detect I and II at 200 and 235 nm for ~100 ng/ml from 5 ml of urine after selective pH extraction. A valid linear calibration curve was claimed to exist over a range of 0.5–10 μg/ml of urine, although no quantitative assays were given (10). A more

Table I—Typical Statistics of HPLC Calibration Curves of I, II, and III in Aqueous Solutions and Plasma [a]

HPLC Procedure, nm of detection	Compound	Range, μg/ml	$s_{C\cdot PHR}$	m	s_m	b	s_b	n	r
I(254)[b]	I	15–111	0.88	88.6	1.0	−4.4	0.8	6	0.9997
	II	7–50	0.34	31.1	0.3	−0.4	0.3	6	0.9998
	III	6–45	0.25	32.2	0.2	−1.9	0.2	6	0.9999
II(254)[c]	I	15–90	1.64	75.5	2.1	−0.3	1.6	5	0.9989
	II	14–81	0.77	55.2	0.8	0.2	0.7	5	0.9997
	III	6–37	0.55	51.3	1.1	−1.5	0.6	5	0.9993
II(232)[c]	I	0.4–2.8	0.038	4.90	0.09	−0.08	0.03	6	0.9990
	II	0.3–2.5	0.065	3.49	0.13	−0.21	0.06	6	0.9971
	III	0.2–1.1	0.035	2.07	0.09	−0.13	0.04	6	0.9969
III(254)[d]	I	4–36	1.16	114.4	5.2	0.88	0.91	5	0.9969
	II	3–31	0.90	63.8	2.5	−0.25	0.73	5	0.9976
IV(232)[e]	I	0.36–2.68	0.049	1.88	0.05	−0.018	0.046	5	0.9989
IV′(232)[e]	I	0.05–0.40	0.0073	0.282	0.008	−0.0026	0.0069	5	0.9989

[a] Statistics are in accordance with $C(\mu g/ml) \pm s_{C\cdot PHR} = (m \pm s_m)\ PHR + b \pm s_b$ from aqueous solutions (HPLC procedure I) and plasma (HPLC procedures II–IV). All values are for concentrations in the final assayed solutions except for IV′ which is for concentrations in the original plasma. The constants m and b are the slope and intercept, respectively, of the regression of concentration (C, μg/ml) on peak height ratio to internal standard (PHR) where $s_{C\cdot PHR}$, s_m, and s_b are standard errors of estimate (μg/ml) (14) of concentration on peak height ratio, of the slope (m), and of the intercept (b), respectively. [b] Degrading buffered solutions of I were diluted to one-sixth the original concentration before assaying in mobile phase solution. [c] Plasma (0.5 ml) denatured with 0.5 ml acetonitrile and the supernatant assayed. [d] Evaporated chloroform extracts of 1.0 ml of plasma were reconstituted in 0.5 ml of aqueous acetonitrile and assayed for I at twice the original plasma concentration. Evaporated 1-butanol extracts of the plasma were reconstituted similarly, and II and III were assayed at twice the original plasma concentration. [e] As in footnote *d* except the compounds were 6.7 times the original 2.0-ml plasma concentration. Plasma components at these low II and III concentrations and at 232-nm detection interfered with their assays.

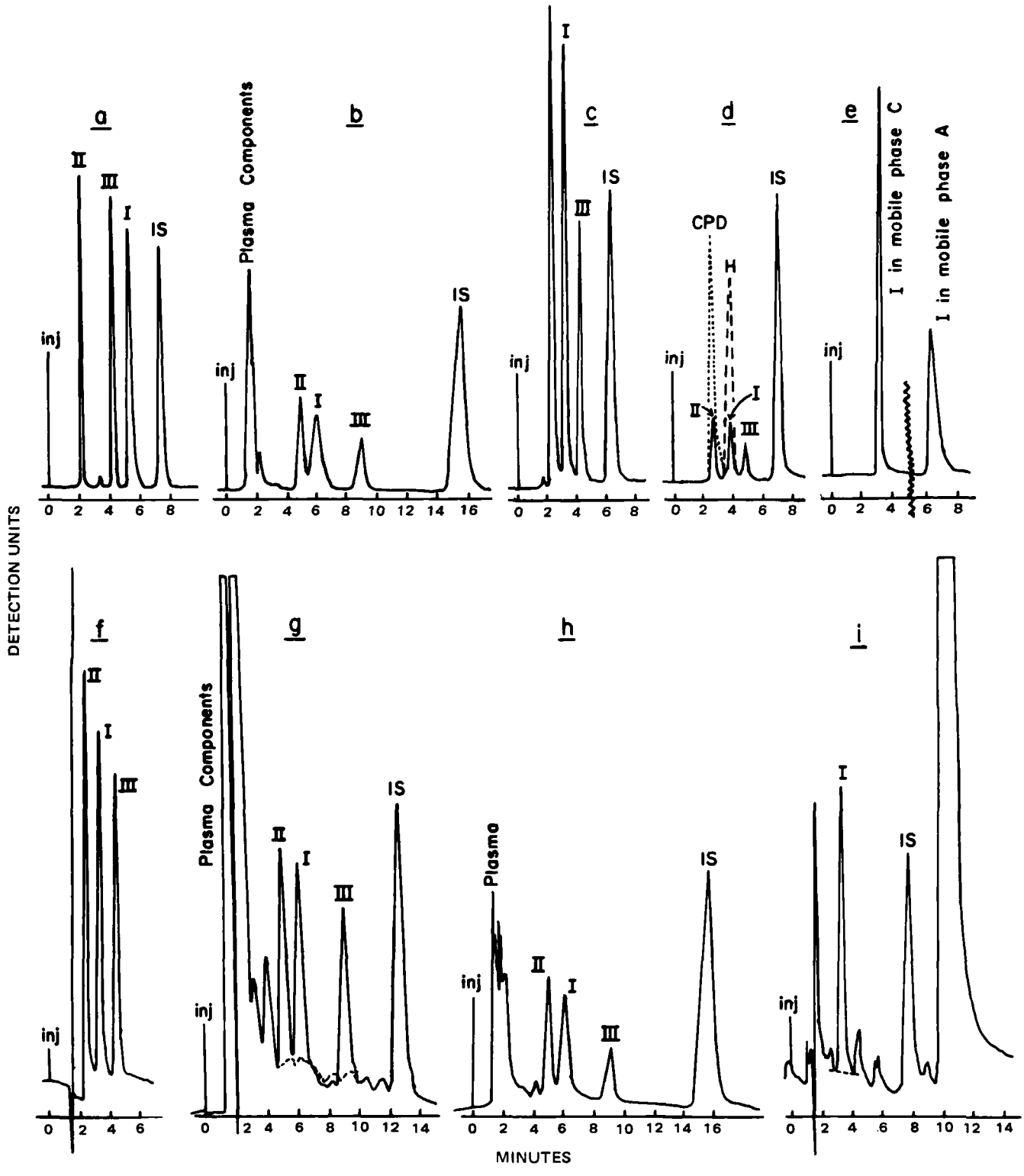

Figure 1—*Examples of reverse-phase HPLC chromatograms at 254-nm detection with 25 μl injected: (a) Aqueous solution containing 2.98 × 10^{-4} M (90.4 μg/ml) I, 1.415 × 10^{-4} M (42.92 μg/ml) II, 3.034 × 10^{-4} M (37 μg/ml) III, and 3.517 × 10^{-4} M (48 μg/ml)* m-*toluic acid (IS) in mobile phase A. (b) Heparinized plasma solution denatured (1:1) with acetonitrile in mobile phase B. The mixture contained 1.98 × 10^{-4} M (60 μg/ml) I, 1.864 × 10^{-4} M (56.5 μg/ml) II, 2.044 × 10^{-4} M (25 μg/ml) III, and 1.057 × 10^{-3} M (144 μg/ml)* o-*toluic acid (IS). (c) Aqueous solution containing 1.65 × 10^{-4} M (50 μg/ml) I, 1.553 × 10^{-4} M (45 μg/ml) II, 1.703 × 10^{-4} M (20.8 μg/ml) III, and 2.968 × 10^{-4} M (40.4 μg/ml)* o-*toluic acid (IS) into mobile phase C. (d) Aqueous solution containing 2.475 × 10^{-5} M (7.5 μg/ml) I, 2.33 × 10^{-5} M (7.07 μg/ml) II, 2.555 × 10^{-5} M (3.12 μg/ml) III, and 2.968 × 10^{-5} M (4.04 μg/ml)* o-*toluic acid (IS) in mobile phase C. The dashed line is the chromatogram for the same composition with heparin (H). The dotted line is the chromatogram for the same composition with citrate phosphate dextrose (CPD) solution USP (5 μl in 2 ml of injected solution. (e) Effect of tetrabutylammonium hydroxide in mobile phase on chromatogram of I. Aqueous solutions of 1.65 × 10^{-4} M (50 μg/ml) I injected into mobile phases A and C, acetonitrile–0.085 M acetate buffer (25:75) (pH 3.6) without and with 0.002 M tetrabutylammonium hydroxide in the acetate buffer, respectively. Examples of reverse-phase HPLC chromatograms at 232 nm detection with 25 μl injected: (f) Aqueous solution*

continued on next page

recent paper claims an HPLC detection limit for I, II, and norcocaine of 1.0 μg/ml of biological fluid from 0.5 ml of sample at 235 nm after extraction at pH 9.0 and reconstitution of the evaporated organic extract in 250 μl of water (11).

In a recent guide to I and metabolite analysis in biological material (12), it was stated that "surprisingly very few papers utilizing this technique for the determination of cocaine and its metabolites have appeared . . ."

One of the HPLC methods presented has an analytical sensitivity in plasma of 15 ng/ml for I.

EXPERIMENTAL

Materials—The following analytical grade materials were used: cocaine hydrochloride[1], benzoylecgonine·4H_2O[1], benzoic acid[2], *m*-toluic acid[3], *o*-toluic acid[3], glacial acetic acid[2], sodium acetate[2], boric acid[4], sodium borate[4], sodium chloride[2], monobasic sodium phosphate[4], dibasic sodium phosphate[2], 1 *M* hydrochloric acid[5], 1 *M* sodium hydroxide[5], 0.4 *M* tetrabutylammonium hydroxide in water[6], acetonitrile[6], chloroform[2], and 1-butanol[4].

Apparatus—A high-performance liquid chromatograph[7] equipped with fixed[8] and variable[9] wavelength UV detectors was used with a reverse-phase μBondapak C_{18} column.

HPLC Procedures—*Procedure I: Kinetics in Aqueous Solution*—The mobile phase (A) acetonitrile–0.085 *M* acetate buffer (25:75) (pH 3.6) with UV detection at 254 nm was used to assay degrading aqueous solutions of I and II with 4.22×10^{-4} *M* *m*-toluic acid as the internal standard. All reaction samples were diluted with acetonitrile and acetate buffer (pH 3.6) which contained the internal standard to give the same composition as the mobile phase, and 25 μl was injected into the chromatograph.

Procedure II: Acetonitrile Denaturation for Higher Concentrations of I in Plasma—Plasma (0.5 ml) was denatured with 0.5 ml of acetonitrile containing 2.113×10^{-4} *M* *o*-toluic acid as internal standard, with vortexing after subsequent centrifugation at 3000 rpm for 10 min. A 25-μl aliquot of the supernatant was injected into the chromatograph with a mobile phase (B) of acetonitrile–0.0002 *M* tetrabutylammonium hydroxide in 0.085 *M* acetate buffer (15:85) (pH 3.63) and UV detection at 254 or 232 nm.

Procedure III: Extraction Procedure for Higher Concentrations of I in Plasma—Plasma (1.0 ml) was extracted twice with 1.00 ml of chloroform. The combined organic extract was evaporated to dryness under nitrogen, reconstituted in 0.5 ml of acetate buffer (pH 3.6)–acetonitrile (1:1) which contained 1.187×10^{-3} *M* *o*-toluic acid as internal standard. Then, 25 μl was injected into the chromatograph to assay I with a mobile phase (C) at 254 nm detection of acetonitrile–0.0002 *M* tetrabutylammonium hydroxide in 0.085 *M* acetate buffer (25:75) (pH 3.63). The extracted plasma was adjusted to pH 3 and again extracted with 10 ml of 1-butanol. The organic extract was evaporated to dryness under nitrogen, reconstituted as above, and 25 μl was injected into the chromatograph to assay II and benzoic acid (III) with mobile phase B at 254 nm detection.

Procedure IV: Extraction Procedure for Lower Concentrations of I in Plasma—Plasma (2.0 ml) was extracted with 3.0 ml of chloroform. The extract (2.0 ml) was evaporated to dryness under nitrogen and reconstituted with 0.2 ml of acetonitrile–acetate buffer (1:3) (pH 3.6) mixture which contained 1.665×10^{-5} *M* *p*-chloroaniline as internal standard. A 25-μl injection was used with mobile phase C for analysis of I at 232 nm detection. Once extracted, the plasma was adjusted to pH 3 and extracted twice with 5 ml of 1-butanol. The combined extracts were taken to dryness, reconstituted as above, and 25 μl was assayed with mobile phase B for II and III. At the low drug concentrations, extracted plasma components interfered with the assay of II. All procedures used flow rates of 2.0 ml/min which gave back pressures of 1800–2100 psi.

Kinetics of Hydrolytic Degradation of I and II—*Acid Hydrolyses*—Aliquots of aqueous solutions of a drug were mixed with appropriate amounts of standardized concentrate to give 0.1, 0.04, and 0.02 *M* HCl solutions that were 1.32×10^{-3} *M* in I or 8.518×10^{-4} *M* in II (Table I). Aliquots (1.5 ml) were put in tightly closed 10-ml vials that were placed in 90, 80, or 70° thermostated oil baths. The vials were withdrawn periodically, ice-cooled, and 0.5 ml of the reaction mixtures was mixed with 2.5 ml of quenching solution containing 4.22×10^{-4} *M* *m*-toluic acid as internal standard. The rates were sufficiently slow such that the time of thermal equilibration did not affect the studies significantly. The quenching solution was an appropriate mixture of acetate buffer–acetonitrile to yield the same ultimate composition of the used mobile phase A in HPLC procedure I.

Alkaline Hydrolyses—Aliquots of aqueous stock solutions of a drug were mixed with thermally preequilibrated appropriate sodium hydroxide solutions (Table I) prepared from a standardized concentrate to obtain 2.472×10^{-3} *M* of I or 8.518×10^{-4} *M* of II. Aliquots (0.5 ml) of the thermostated samples were pipeted periodically into 2.5 ml of a quenching solution that contained acetate buffer, acetonitrile, and hydrochloric acid for neutralization of excess sodium hydroxide and internal standard and was 4.22×10^{-4} *M* in *m*-toluic acid. The HPLC procedure I was used for the assay.

Solvolysis Studies at Intermediate pH-Values—Acetate (pH 3.98–5.67), phosphate (pH 6.22–7.25), and borate (pH 7.72–11.85) buffers were prepared with ionic strengths of 0.1 adjusted with sodium chloride. The buffer solutions were preequilibrated in a constant-temperature bath before addition of appropriate amounts of stock solutions of I or II to obtain concentrations of 1.32×10^{-3} *M* and 8.51×10^{-4} *M* for I and II, respectively. Aliquots (0.5 ml) were removed periodically into 2.5 ml of quenching solution which contained 4.22×10^{-4} *M* *m*-toluic acid as internal standard to obtain the same composition as the HPLC mobile phase A. HPLC Procedure I was used for the assay.

Buffer Catalysis—Kinetic studies were conducted at several concentrations of buffers at a pH equal to the pK_a of appropriate buffer and constant ionic strength 0.1 (Table I). Additional studies at different pH values and concentrations of acetate buffer were effected. No significant buffer catalysis was observed in any of the buffers.

Potentiometric Determination of $pK_{a'}$ Values of I and II—Compound I or II (0.00017 mole) was dissolved in 5 ml of 0.1 *M* HCl, diluted with 20 ml of deionized water, and titrated potentiometrically with 0.1 *M* NaOH. The blank solutions, without I or II, were titrated similarly. The $pK_{a'}$ values were estimated from the plots of the difference between the number of milliliters of titer necessary to bring both blank solutions and solutions containing a drug to the same pH value (13). The $pK_{a'}$ values of I were estimated at several temperatures by half neutralizing solutions of I maintained at those temperatures and measuring the pH values as a function of time and extrapolating pH values back to time zero. This method was complicated by the 10–20 sec necessary to obtain electrode equilibration and the relatively fast degradation of I at these pH values and higher temperatures.

Kinetics of Degradation of Higher Concentrations of I in Plasma—An aliquot (0.4 ml) of an aqueous solution of 3.3×10^{-3} *M* I hydrochloride was evaporated under nitrogen to dryness, and the residue was mixed with 15 ml of heparinized fresh dog plasma, thermally equil-

[1] NIDA, 1140 Rockville Pike, Rockville, MD 20852.
[2] Malinckrodt Chemical Works, St. Louis, MO 63160.
[3] Eastman Kodak Co., Rochester, NY 14650.
[4] J. T. Baker Chemical Co., Phillipsburg, NJ 08865.
[5] Ricca Chemical Co., Arlington, TX 76012.
[6] Fisher Scientific Co., Chemical Manufacturing Division, Fair Lawn, NJ 07410.
[7] Model M-6000 A solvent delivery system and model U6K injector, Waters Associates, Milford, MA 01757.
[8] Model 440 absorbance detector, Waters Associates, Milford, MA 01757.
[9] Model 450 variable-wavelength UV detector, Waters Associates, Milford, MA 01757.

continued
containing 9.075×10^{-6} M (2.75 μg/ml) I, 8.54×10^{-6} M (2.6 μg/ml) II, and 9.368×10^{-6} M (1.14 μg/ml) III into mobile phase C. (g) Plasma obtained with citrate phosphate dextrose USP as anticoagulant and denatured 1:1 with acetonitrile. The mixture containing 9.075×10^{-6} M (2.75 μg/ml) I, 8.54×10^{-6} M (2.6 μg/ml) II, 9.368×10^{-6} M (1.14 μg/ml) III, and 4.14×10^{-5} M (5.28 μg/ml) p-chloroaniline (IS) was injected into mobile phase B after denaturation (1:1) with acetonitrile. (h) Plasma (1.0 ml) with 1.087×10^{-4} M II, 1.155×10^{-4} M I, and 1.192 M III was extracted with 2 ml of chloroform, adjusted to pH 3, and extracted with 10 ml butanol. The combined extracts were evaporated, reconstituted in 1.0 ml of mobile phase containing 5.94×10^{-4} M o-toluic acid (IS) and 25 μl was injected with mobile phase B. (i) Plasma (2.0 ml) at 0.50 μg/ml of I was extracted with 3.0 ml chloroform. An aliquot (2.0 ml) of extract was evaporated, the residue reconstituted in 0.2 ml of mobile phase, and 25 μl of 7.58×10^{-6} M solution (2.3 μg/ml) injected into mobile phase C (Procedure IV). The dashed line is for a sample treated similarly without I. The internal standard (IS) was 2.22×10^{-5} M p-chloroaniline in the injected sample.

Table II—Apparent Partition Coefficients for I (C_{org}/C_{buffer}) with Various Organic Phases

pH	Diethyl Ether	Hexane	Benzene	Methylene Chloride	Chloroform
10.7	161	46	—	220	>200
9.0	159	32	212	>200	237
8.2	22	7.5	135	—	185
5.9	0.023	0.07	1.6	4.0	5.5
3.9	—	—	0.04	0.22	0.30

ibrated at the body temperature of the dog (38.9°) to give an 8.8×10^{-3} *M* (299 μg/ml) or 8.8×10^{-4} *M* (29.9 μg/ml) solution. The residues were assayed with time by Procedures II and III, respectively.

Kinetics of Degradation of Lower Concentrations of I in Plasma—Since heparin interfered with the use of Procedure IV for the assay of low concentrations of cocaine, a citrate, phosphate, and dextrose solution USP[10] was used as the anticoagulant for assays of I in plasma at an initial concentration of 1.471×10^{-6} *M* (0.5 μg/ml) and 38.9° by this procedure. The spiked plasma was prepared in the same manner as described earlier.

Kinetics of Degradation of II in Plasma—An aliquot (0.35 ml) of an acetonitrile solution of 3.105×10^{-2} *M* II·4H_2O was evaporated under nitrogen to dryness, and the residue was mixed with 15 ml of heparinized fresh dog plasma to give a 7.245×10^{-4} *M* solution. Aliquots (0.5 ml) at 38.9° were periodically mixed with 0.5 ml of acetonitrile supernatant to be assayed by Procedure II.

Partition Studies as Function of pH—Partition studies between appropriate volume ratios of water-saturated organic solvent and buffer solutions of various pH values were effected by shaking mixtures containing I·HCl or II. Higher relative volumes of organic phase were used at the lower pH values of the buffer and lower volumes of organic solvent at higher pH values in the cocaine studies. Higher relative volumes of organic phase were used in the studies of II in each experiment. Aliquots of the separated organic phases were evaporated under nitrogen to dryness and assayed by HPLC Procedure I after reconstitution in the mobile phase. The aqueous phases were adjusted to the composition of the mobile phase and assayed similarly.

Red Blood Cell–Plasma and Buffer Partitioning—Aliquots of a stock solution of I hydrochloride (0.02 mg/ml) were evaporated to dryness and reconstituted with whole blood with an hematocrit of 41.5 or with a red blood cell suspension in plasma–water or buffer with an hematocrit of 32.5 and maintained at 38.9°. After 1 and 2 hr, the vials were centrifuged at 3000 rpm, and 0.5 ml of plasma or buffer layer was extracted with 1.0 ml of chloroform. An aliquot of the chloroform (0.75 ml) was evaporated and reconstituted in 1 ml of acetonitrile–0.085 *M* acetate buffer (25:75) (pH 3.6), and 25 μl was injected into mobile phase C for HPLC detection at 232 nm.

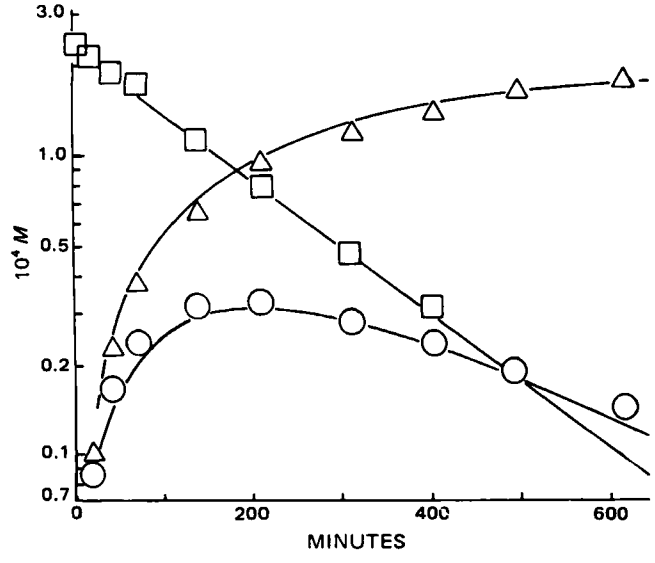

Figure 2—*Semilogarithmic plots of I, II, and III against time on I solvolysis in hydrochloric acid solutions. The curves through the data were calculated from the equations given in the text based on the kinetic constants given in the tables. The specific conditions of the kinetic study were for an initial concentration of 1.32×10^{-3} M I at 80.1° in 0.04 M HCl (pH 1.48). The initial theoretical concentration of the assayed quenched solution was 2.21×10^{-4} M in I. Key: (□) I; (○) II; (△) III.*

[10] McGaw Blood Products, McGaw Laboratories, Division of American Hospital Supply Corporation, Irvine, CA 92714.

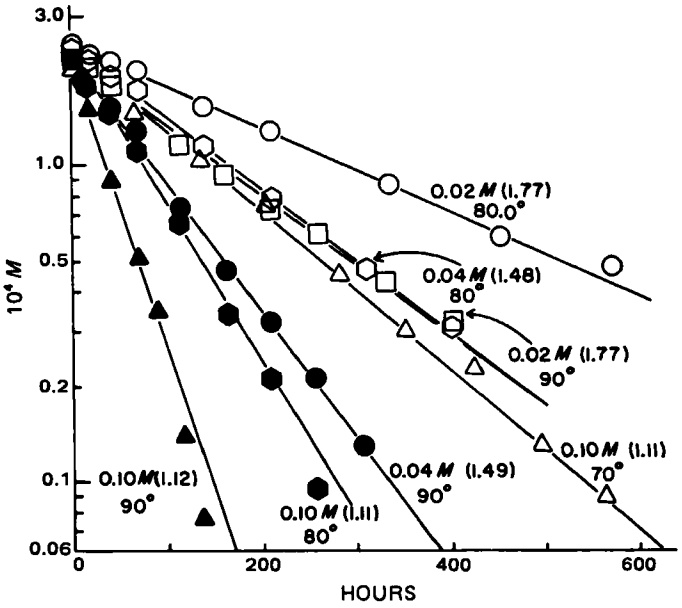

Figure 3—*Semilogarithmic plots of I in its quenched solution against time for its solvolysis in the labeled hydrochloric acid solutions. Calculated pH values are given in parentheses.*

Protein Binding by Ultrafiltration—Fresh ultrafiltration membrane cones[11] were used to filter 4 ml of plasma–water and plasma containing 1 μg/ml of I with centrifugation at 1000 rpm. The solutions were

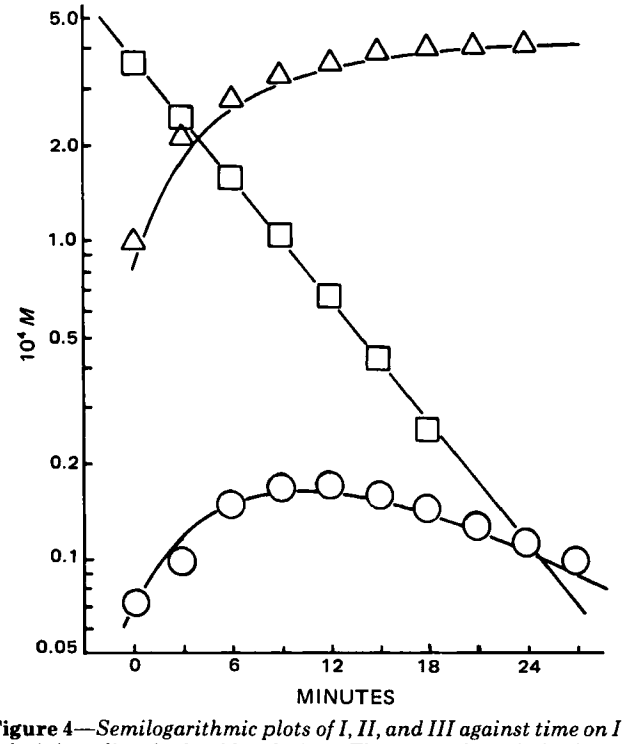

Figure 4—*Semilogarithmic plots of I, II, and III against time on I solvolysis in sodium hydroxide solutions. The curves through the data were calculated from the equations given in the text based on the kinetic constants given in the tables. The specific conditions of the kinetic study were for an initial concentration of 2.70×10^{-3} M I at 30.0° in 0.0373 M NaOH (pH 12.25). The initial theoretical concentration of the assayed quenched solution was 4.50×10^{-4} M in I. Key: (□) I; (○) II; (△) III.*

[11] Membrane filter cones 2100 CF 50, Amicon Co., Lexington, MA 02173.

Table III—First-Order Rate Constants (k, sec^{-1}) [a]

[NaOH][b]	Temperature	pH[c]	10^5k	10^5k_1	10^5k_2	10^5k_3
0.0884	15.1	13.18	208	12.5	80.0	195
0.0884	19.6	13.01	268	16.1	96.0	252
0.0884	30.0	12.67	534	32.1	160	502
0.0773	30.0	12.61	451	—	—	—
0.0573	30.0	12.50	382	20.2	115	362
0.0373	30.0	12.33	242	17.0	92.5	225
0.0170	30.0	12.02	101	12.7	61.0	87.1
0.0884	39.7	12.37	984	59.1	300	925
[HCl]						
0.100	70.0	1.11	0.161	0.0643	0.126	0.0965
0.020	80.0	1.77	0.0847	0.0381	0.0836	0.0467
0.040	80.0	1.48	0.144	0.0576	0.127	0.0864
0.100	80.0	1.11	0.319	0.128	0.246	0.192
0.020	90.0	1.77	0.140	0.0629	0.165	0.0768
0.040	90.0	1.49	0.265	0.111	0.240	0.154
0.100	90.0	1.12	0.588	0.223	0.491	0.335

[a] Rate constants for overall hydrolysis of I, for hydrolysis to II (k_1, sec^{-1}), and to IV (k_3, sec^{-1}) and for the hydrolysis of II (k_2, sec^{-1}) to ecgonine in hydrochloric acid and sodium hydroxide solutions (Scheme I). [b] Final compositions. Sufficient alkali was added to neutralize the added I hydrochloride. [c] The pH values for [NaOH] and [HCl] solutions were calculated from $pH = pK_w + \log f_{NaOH}[NaOH]$ and $pH = -\log f_{HCl}[HCl]$, respectively, from the pK_w values and activity coefficients, f_{NaOH} and f_{HCl}, available in the literature (15) for the designated temperatures, $pK_w = 2715(1/T) + 4.87$.

filtered, and the filtrates were assayed by the described HPLC procedures. Cones pre-equilibrated by filtering 2.5 ml of 6.0 ml of phosphate buffer (pH 7.5) containing 1 and 2 μg/ml, respectively, of I were also used. The same amount of plasma with the same concentrations of I were filtered through the respective cones, and the filtrate was assayed.

RESULTS AND DISCUSSION

HPLC Assays—The specific HPLC assays developed for cocaine (I) and its solvolysis products, benzoylecgonine (II) and benzoic acid (III), were applied to kinetic studies of the solvolysis of I and II and to partition studies of these compounds. Statistics of typical calibration curve regressions are given in Table I; HPLC chromatograms are given in Fig. 1. The analytical sensitivities ($2 \times s_{C\text{-}PHR}$) of 0.5–1.6 μg/ml (Procedure I, Table I; Fig. 1a) with UV detection at 254 nm with mobile phase A, of 1.0–3.0 μg/ml (Procedure II, Table I; Fig. 1b) were modified to 70–120 ng/ml by the use of a variable wavelength detector of 232 nm with a modified mobile phase B (Fig. 1g) or C (Fig. 1f; Procedure II, Table I) containing 0.0002 M tetrabutylammonium hydroxide in the 0.085 M acetate buffer.

Tetrabutylammonium hydroxide in mobile phase C increased the peak height sensitivity of the assay of I by decreasing its retention time (Fig. 1e). A concentration of 0.0002 M tetrabutylammonium hydroxide decreased the retention time of I from 6.6 to 3.2 min and 0.0004 M to 2.4 min. The tetrabutylammonium cation blocks adsorption sites on the column from I and effectively lowers the retention volume of I. The peak heights and retention times of the acidic II (2.3 min) and III (4 min) at pH 3.63 of the mobile phases, close to the pH of maximum stability of I and II, were not significantly affected by the tetrabutylammonium hydroxide.

Mobile phase B (Figs. 1b, 1g, and 1h) was advantageous in the assay of plasma solutions, in that plasma component peaks did not interfere with those of I and II in this system as they did in mobile phases A and C (Fig. 1i). The plasma component peaks did not interfere with the cocaine assay using mobile phase C in the extraction HPLC procedures III and IV (Fig. 1i), although some interferences were observed in C but not B at low concentrations of II. The sequential extraction procedures of III and methylecgonine (IV) permitted the selective assay of II in mobile phase B where there was no interference.

The retention times of heparin and I were similar in mobile phases B and C (Fig. 1d shows mobile phase C). Thus, the noninterfering citrate phosphate dextrose solution USP was used as the anticoagulant in plasma studies for the assay of low concentrations of I in mobile phase C (Fig. 1d). In this mobile phase, the anticoagulant, citrate phosphate dextrose solution USP, interfered with the peak of II (Fig. 1d) but did not interfere when mobile phase B was used (Fig. 1h).

The use of the developed extraction procedures with reconstitution into small volumes of the dried extracts gives analytical sensitivities from plasma of 15 ng/ml (Procedure IV and IV′, Table I) for I.

The apparent partition coefficients for I into several organic solvents are given in Table II for several pH values. All of the solvents listed showed potential complete extractions of I above pH 8.0. Chloroform appeared best suited for extraction at plasma pH values.

Compound II, at a pH of 6.32 where it exists as the zwitterion, had the following partition coefficients in the designated solvents: 0.4, ethyl acetate–acetonitrile (1:1); 0.79, isobutyl alcohol; and 0.87, *sec*-butyl alcohol. The partition coefficients for 1-butanol at pH 7.67, 6.32, and 3.89 were 1.02 ± 0.02 and were 0.30 ± 0.1 for *n*-butyl alcohol–chloroform (1:3). The partition coefficients for chloroform and methylene dichloride extraction of II were 0.12 ± 0.01 at pH 4, 6, 8, 9, and 11. Thus, 1-butanol was the most effective solvent for extraction of II.

These partition studies served as the basis for designing the sequential extraction of I and its metabolites. A primary extraction of I with limited amounts of chloroform at >pH 7 would remove negligible amounts of II, which could be reasonably extracted subsequently with 1-butanol. At pH 3, III would be readily extracted as well.

Kinetics of Solvolysis of I and II—At constant pH, I degrades by an apparent first-order process. Representative semilogarithmic plots of concentrations, C, against time are given for hydrochloric acid solutions (Figs. 2 and 3), sodium hydroxide solutions (Figs. 4 and 5), and buffers (Figs. 6 and 7), where the apparent first-order rate constants, k, were obtained from the slopes in accordance with:

$$\log C = -\frac{k}{2.303}t + \log C_0 \qquad \text{(Eq. 1)}$$

where C and C_0 are the concentrations at time t and time zero, respectively. These k-values are listed in Tables III and IV.

The pH values of the degrading buffer solutions were determined experimentally at the temperature of the study. The pH values for hydrochloric acid solutions were calculated from:

$$pH = -\log \gamma[HCl] \qquad \text{(Eq. 2)}$$

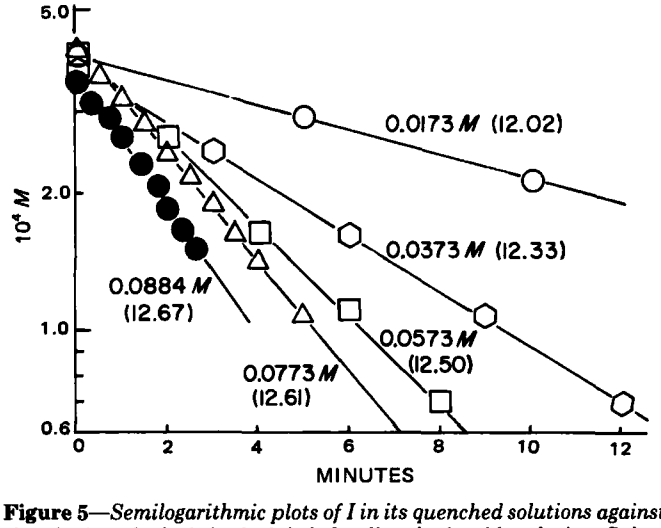

Figure 5—*Semilogarithmic plots of I in its quenched solutions against time for its solvolysis in the labeled sodium hydroxide solution. Calculated pH values at 30.0° are given in parentheses.*

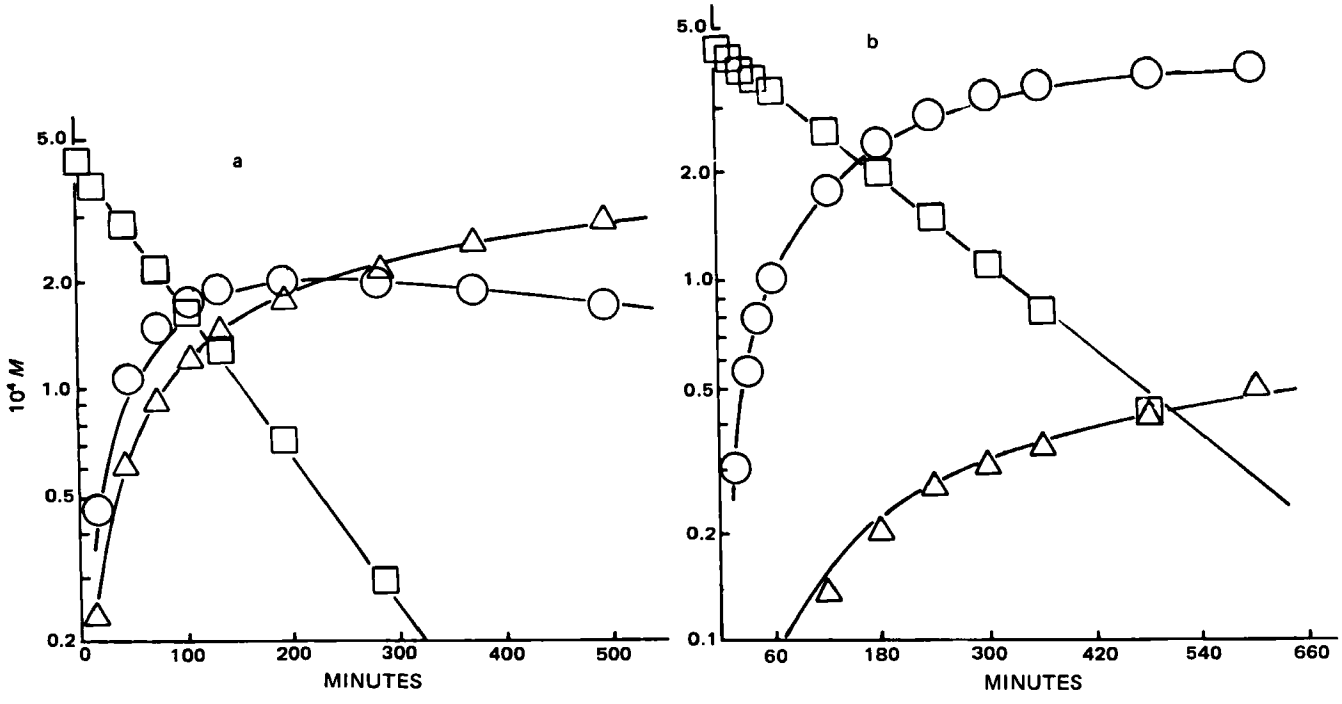

Figure 6—*Example of semilogarithmic plots of I, II, and III against time on I solvolysis in buffered solutions. The curves through the data were calculated from the equations given in the text based on the kinetic constants given in the tables. The specific conditions of the kinetic studies were for initial concentration of 2.65 × 10^{-3} M I at 30.0° at a) pH 10.33 and b) pH 9.09. The initial theoretical concentrations of the assayed quenched solutions were 4.41 × 10^{-4} M in I. Key: (□) I; (○) II; (△) III.*

where γ is the mean activity coefficient for the hydrochloric acid solutions. For sodium hydroxide solutions:

$$\text{pH} = pK_w - \text{pOH} = pK_w + \log \gamma[\text{NaOH}] \qquad \text{(Eq. 3)}$$

where γ is the mean activity coefficient for the sodium hydroxide solution (15) and values of pK_w are $-\log K_w$ where K_w is the hydrolysis constant for water.

In a similar manner, some direct measurements of the first-order rate constants, k_2, for II solvolysis to ecgonine (V) and III, (Scheme I) were determined. Examples of the semilogarithmic plots of concentrations, C, against time are given in Fig. 8, and the determined rate constants k_2 at the specified conditions are given in Table V.

Determination of Rate Constants in the Sequential Hydrolysis of I—The overall rate constant, k, for the hydrolysis of I is the sum of the separate constants, k_1 and k_3, for the routes to II and III plus IV, respectively (Scheme I):

$$k = k_1 + k_3 \qquad \text{(Eq. 4)}$$

If I were hydrolyzed solely to II, *i.e.*, $k_3 = 0$, the concentration of generated II would be (16):

$$[\text{II}]' = [\text{I}]_0 \frac{k}{k_2 - k}(e^{-kt} - e^{-k_2 t}) \qquad \text{(Eq. 5)}$$

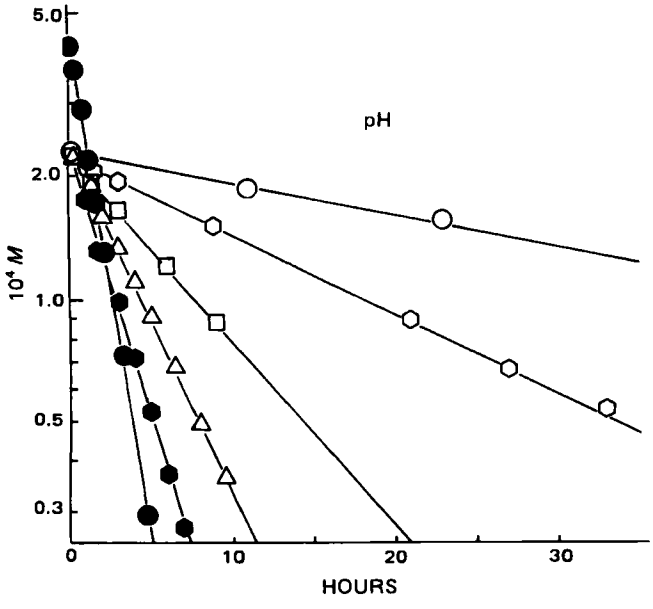

Figure 7—*Semilogarithmic plots of I in its quenched solutions against time for its solvolysis in the buffer at 30.0°. Key: (●) pH 10.33; (●) pH 8.94; (△) pH 8.55; (□) pH 8.15; (○) pH 7.72; (○) pH 7.25.*

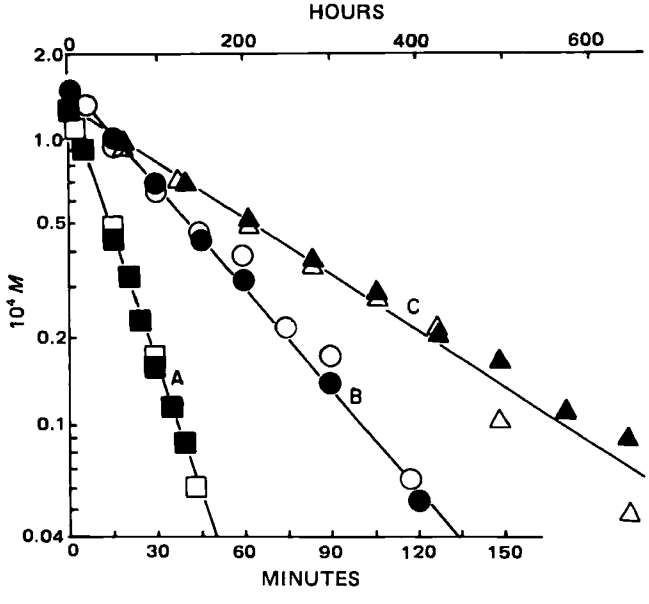

Figure 8—*Semilogarithmic plots of II concentrations (c_0 = 1.42 × 10^{-4} M) in quenched solutions against time. The solid symbols are for plots of II against time. The open symbols are for the difference plots of III, $[III]_\infty - [III]$ against time: A) 0.060 M NaOH, pH 12.32 at 30.0° against time scale in minutes; B) borate buffer, pH 8.92 at 80.0° against time scale in minutes; C) 0.04 M HCl solution, pH 1.41 at 80.0° against time scale in hours. The initial concentration of II in the reaction mixture was 8.52 × 10^{-4} M.*

Table IV—First-Order Rate Constants (k, sec^{-1}) [a]

Buffer	Temperature	pH	10^5k	10^5k_1	10^5k_2	10^5k_3
Borate	30.0	11.85	105	—	—	—
Borate	30.0	11.38	52.7	10.5	27.0	42.2
Borate	30.0	10.33	15.6	9.53	2.08	6.10
Borate	30.0	9.63	10.2	9.15	0.417	1.02
Borate	30.0	9.09	7.74	7.12	0.133	0.619
Borate[b]	30.0	9.14	10.1	8.96	0.150	1.11
Borate[c]	30.0	9.15	10.2	—	—	—
Borate[d]	30.0	9.14	9.81	—	—	—
Borate	30.0	8.94	8.26	7.43	0.0980	0.826
Borate	30.0	8.55	5.83	5.13	0.0400	0.700
Borate	30.0	8.15	2.92	2.63	0.0160	0.292
Borate	30.0	7.72	1.25	1.12	0.0054	0.125
Phosphate[e]	30.0	7.25	0.497	0.447	0.0019	0.50
Phosphate[f]	30.0	7.26	0.500	—	—	—
Phosphate[g]	30.0	7.27	0.507	—	—	—
Phosphate	70.0	6.22	4.37	3.94	0.0833	0.43
Phosphate	80.0	6.26	11.4	10.2	0.136	1.2
Phosphate	90.0	6.25	37.1	33.4	0.250	3.71
Acetate	80.0	5.23	1.78	1.60	0.0540	0.18
Acetate	80.0	4.70	0.362	—	—	—
Acetate	80.0	4.38	0.241	0.224	0.039	0.017
Acetate[h]	90.0	5.65	7.37	6.34	0.0917	1.03
Acetate[i]	90.0	5.65	7.22	—	—	—
Acetate	90.0	5.24	3.64	3.20	0.0840	0.44
Acetate[j]	90.0	4.70	1.30	1.14	0.0833	0.16
Acetate[k]	90.0	4.69	0.985	—	—	—
Acetate[l]	90.0	4.69	0.966	—	—	—
Acetate[l]	90.0	4.69	0.812	—	—	—
Acetate	90.0	4.37	0.640	0.557	0.0833	0.083
Acetate[m]	90.0	4.06	0.293	0.258	0.080	0.035
Acetate[n]	90.0	4.05	0.275	—	—	—
Acetate[o]	90.0	4.04	0.242	—	—	—
Acetate[p]	90.0	4.06	0.201	—	—	—

[a] Rate constants for overall hydrolysis of I, for hydrolysis to II (k_1, sec^{-1}) and IV (k_3, sec^{-1}) and for the hydrolysis of III (k_2, sec^{-1}) to ecgonine in buffer solutions at 0.1 ionic strength (Scheme I). [b] The composition of the borate buffer in the reaction mixture was 0.1 *M* NaH_2BO_3 + 0.1 *M* H_3BO_3. [c] The borate buffer in footnote *b* was diluted 1:1 with 0.1 *M* NaCl. [d] The borate buffer in footnote *b* was diluted 1:3 with 0.1 *M* NaCl. [e] The composition of the phosphate buffer in the reaction mixture was 0.017 *M* NaH_2PO_4 + 0.017 *M* Na_2HPO_4 + 0.033 *M* NaCl. [f] The phosphate buffer of footnote *e* was diluted 1:1 with 0.1 *M* NaCl. [g] The phosphate buffer of footnote *e* was diluted 1:3 with 0.1 *M* NaCl. [h] The composition of the acetate buffer in the reaction mixture was 0.011 *M* CH_3COOH + 0.089 *M* CH_3COONa + 0.011 *M* NaCl. [i] The acetate buffer of footnote *h* was diluted 4:1 with 0.1 *M* NaCl. [j] The composition of the acetate buffer in the reaction mixture was 0.05 *M* CH_3COOH + 0.05 *M* CH_3COONa + 0.05 *M* NaCl. [k] The acetate buffer of footnote *j* was diluted 1:1 with 0.1 *M* NaCl. [l] The acetate buffer of footnote *j* was diluted 1:3 with 0.1 *M* NaCl. [m] The composition of the acetate buffer in the reaction mixture was 0.083 *M* CH_3COOH + 0.017 *M* CH_3COONa + 0.083 *M* NaCl. [n] The acetate buffer of footnote *m* was diluted 4:1 with 0.1 *M* NaCl. [o] The acetate buffer of footnote *m* was diluted 1:1 with 0.1 *M* NaCl. [p] The acetate buffer of footnote *m* was diluted 1:4 with 0.1 *M* NaCl.

where $[I]_0$ is the initial concentration of I and [II]′ is the predicted concentration of II on the presumption that the sole route of hydrolysis is:

$$I \xrightarrow{k} II + CH_3OH \xrightarrow{k_2} III + IV$$

However, if IV and III were also products of the hydrolysis of I, the actual concentration of II, would be (9, 17):

$$[II] = [I]_0 \frac{k_1}{k_2 - k}(e^{-kt} - e^{-k_2t}) \qquad \text{(Eq. 6)}$$

where

$$k_1/k = [II]/[II]' \qquad \text{(Eq. 7)}$$

Thus, the ratios of the observed experimental concentrations of II, [II], to the concentrations generated by Eq. 5 for a given time [II]′, will be constant, and the k_1 and k_3 values can be estimated from Eqs. 7 and 4, respectively.

The apparent first-order rate constant, k_2, for the hydrolysis of II could be obtained from the terminal slope of the semilogarithmic plots of its generation from I with time (Figs. 2, 4, and 6) or from the direct kinetic studies of II (Fig. 7, Table V).

An alternate method to deduce k_1 and k_2 values is to best fit Eq. 6 to the time-course data of experimentally determined concentrations of II with appropriate adjustments of k_1 and k_2 as was done in Figs. 2, 4, and 6 where the curves drawn through the data were drawn in accordance with Eqs. 1 and 6 for I and II, respectively. The appropriate constants are listed in Tables III–V. The calculated time curve for [III] was calculated from:

$$[III] = [I]_0 - [II] \qquad \text{(Eq. 8)}$$

The data show that, contrary to prior implications (5), the route to II is not the only route of hydrolysis of I at pH >1.0.

The fraction through the route for II on hydrogen ion attack on protonated I <pH 2.0 is 0.4 (Fig. 2 and Table III). The fraction through this route for hydroxide ion attack on neutral I >pH 11.5 is only 0.06 (Fig. 4, Table III), whereas the hydroxide attack on protonated I between pH 4 and 10 gives a fraction of 0.90 (Fig. 6, Table IV). There are intermediate fractions between the stated pH ranges.

Log k–pH Profiles for I—The log k–pH profiles (6) for the overall hydrolysis of I (Fig. 9), the log k_1–pH profiles for the hydrolysis of I through II (Fig. 10), and the log k_3–pH profiles for the hydrolysis of I through IV and III (Fig. 11) are fitted in accordance with:

$$k_i = (k'_{OH})_i\, a_{OH}\, [I] + (k_{OH})_i\, a_{OH}[IH^+] + (k_H)_i\, a_{H^+}\, [IH^+] \qquad \text{(Eq. 9)}$$

where k_i is k, k_1, or k_3; a_{H^+} and a_{OH^-} are the respective activities of the hydrogen and hydroxyl ions; [I] and $[IH^+]$ are the respective concentrations of neutral and protonated I; $(k'_{OH})_i$ is the specific bimolecular rate constant for hydroxide ion attack on neutral I; $(k_{OH})_i$ is the specific bimolecular rate constant for hydroxide ion attack on protonated I; and $(k_H)_i$ is the specific bimolecular rate constant for hydrogen ion attack on protonated I.

The acid branches of the log k_i–pH profiles can be fitted to:

$$\log k_i = \log (k_H)_i - pH \qquad \text{(Eq. 10)}$$

to obtain estimates of $(k_{H^+})_i$.

The alkaline branches are characterized by:

$$k_i = (k'_{OH})_i\, f_I\, a_{OH} + (k_{OH})_i\, f_{(IH^+)}\, a_{OH} \qquad \text{(Eq. 11)}$$

where f_I is the fraction of I concentration that is the neutral species, and $f_{(IH^+)}$ is the fraction that is the protonated species. These fractions can be calculated from the known pH, pK'_a, and pK_w values from:

$$f_I = \frac{K'_a}{K'_a + a_{H^+}} \qquad \text{(Eq. 12)}$$

$$f_{(IH^+)} = \frac{a_{H^+}}{K'_a + a_{H^+}} \qquad \text{(Eq. 13)}$$

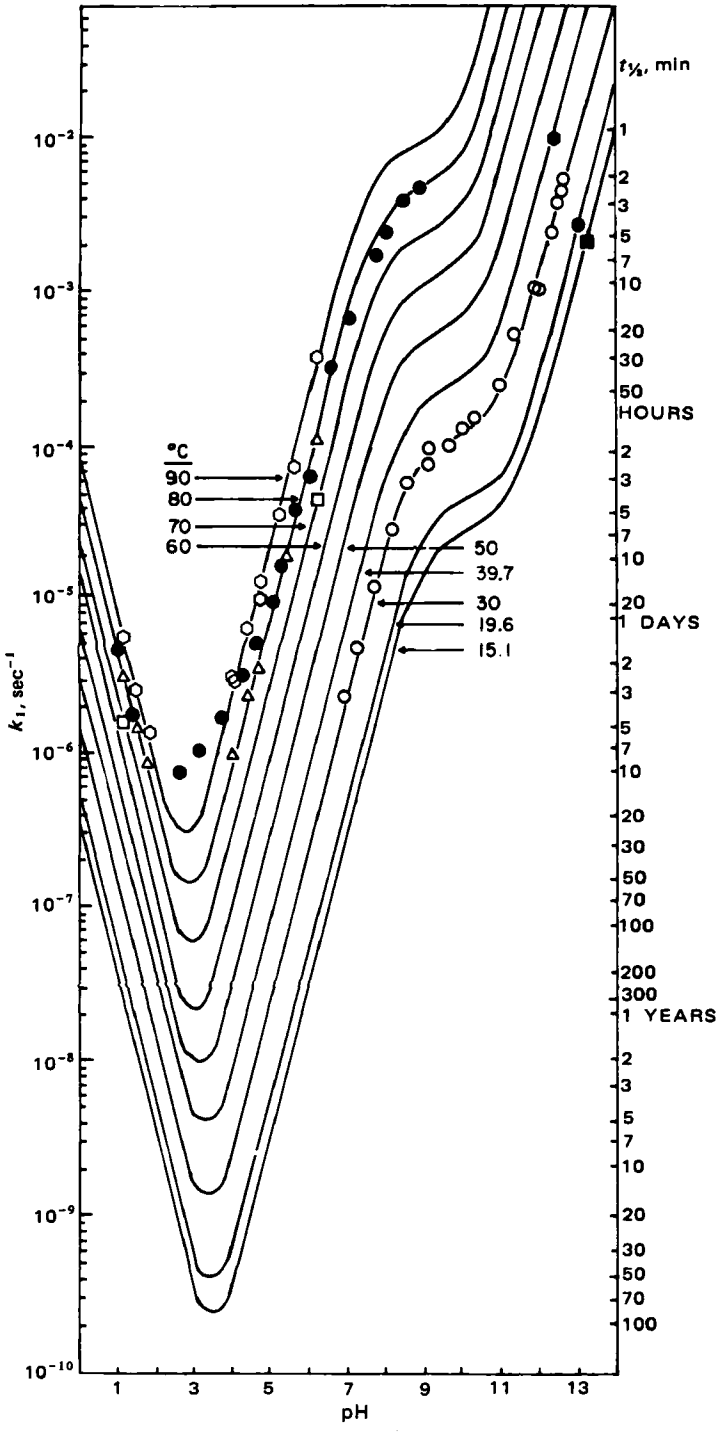

Figure 9—*Fitted and predicted log* k–*pH profiles for the overall hydrolyses of I at the designated temperatures. The fits and predictions are in accordance with:* $k = k_{H}a_{H^+} + k_{OH}\,[K_w/(K'_a + a_{H^+})] + k'_{OH}\,[K'_aK_w/(K'_a + a_{H^+})]$ *and* $\ln k_j = \ln P - 10^3\,(\Delta H_a/R)(1/T)$ *where the pertinent parameters are listed in Table VI,* ΔH_a *is in kcal/mole,* $a_{H^+} = 10^{-pH}$ *and* T *is in degrees Kelvin. The solid symbols are previously reported data (Ref. 5) for rate constants obtained at 80° plotted against the stated pH values for the various buffer solutions.*

where $a_{H^+} = 10^{-pH}$, $K_w = 10^{-pK_w}$ and $K'_a = 10^{-pK'_a}$. Since $K_w = a_{H^+}a_{OH^-}$, Eq. 11 can be modified to:

$$k_i = (k'_{OH})_i \frac{K'_a K_w}{(K'_a + a_{H^+})a_{H^+}} + (k_{OH})_i \frac{K_w}{(K'_a + a_{H^+})} \qquad \text{(Eq. 14)}$$

which was used to fit the alkaline branches of the log k_i–pH profiles of Figs. 9–11 with the parameters listed in Table VI.

The potentiometrically determined pK'_a of I was 8.81 at 25°. The apparent pK'_a values obtained by extrapolation of the pH-values of half-neutralization back to time zero were 8.81 at 25°, 8.70 at 30°, 8.30 at 60°, 8.19 at 70°, 8.04 at 80°, and 7.95 at 90°. These pK'_a values can be characterized by $1429(1/T) + 4.02$, where T is degress Kelvin but are suspect, since degradation of I at these pH-values and temperatures were fast. When the kinetic pK'_a values of best fit at 30 and 80° were used to esti-

Table V—First-Order Rate Constants (k_2, sec^{-1}) from Direct Studies of the Hydrolysis of II

[NaOH]	Temperature	pH[a]	10^5k_2
0.0992	30.0	12.71	154
0.0592	30.0	12.51	113
0.0392	30.0	12.34	95.0
0.0192	30.0	12.06	64.2
0.0192	40.0	11.76	132
0.0192	50.0	11.49	280
0.0192	60.0	11.24	516
[HCl]			
0.0992	70.0	1.12	0.126
0.0992	80.0	1.12	0.249
0.0392	80.0	1.49	0.127
0.0192	80.0	1.79	0.0836
0.0992	90.0	1.12	0.491
0.0392	90.0	1.50	0.256
0.0192	90.0	1.79	0.165
Buffer			
Borate	30.0	10.33	1.65
Borate	30.0	9.59	0.474
Borate	30.0	9.25	0.190
Borate	30.0	9.09	0.126
Borate	80.0	8.92	45.2
Borate	90.0	8.94	93.9
Acetate	90.0	5.27	0.883
Acetate	90.0	4.43	0.695

[a] The pH-values for [NaOH] and [HCl] solutions were calculated from $pH = pK_w + \log f_{NaOH}[NaOH]$ and $pH = -\log f_{HCl}[HCl]$, respectively, from the pK_w values and activity coefficients, f_{NaOH} and f_{HCl}, available in the literature (15) for the designated temperatures.

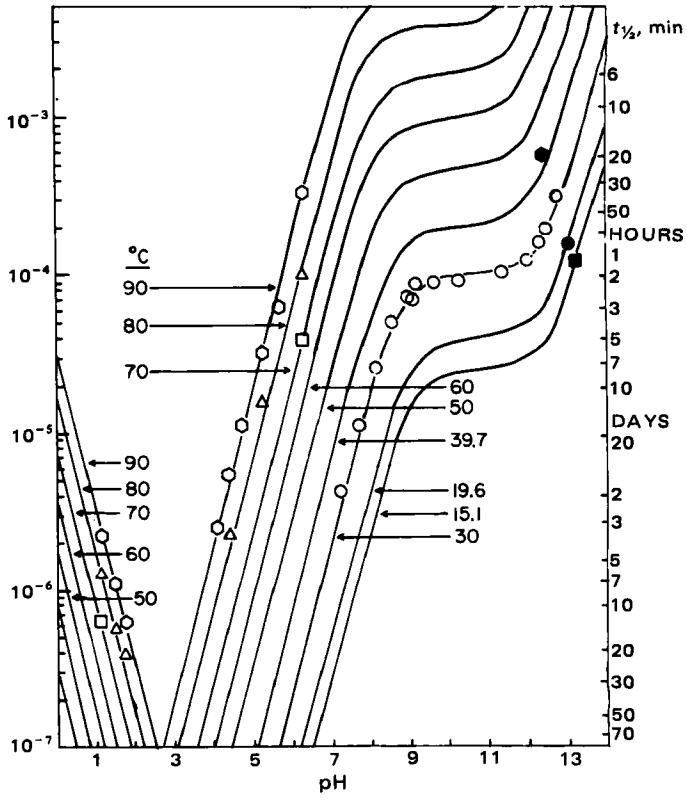

Figure 10—*Fitted and predicted log* k_1–*pH profiles for the hydrolysis of I to II at the designated temperatures. The fits and predictions are in accordance with:* $k_1 = (k_H)_1a_{H^+} + (k_{OH})_1\,[K_w/(K'_a + a_{H^+})] + (k'_{OH})_1\,K'_aK_w/[(K'_a + a_{H^+})a_{H^+}]$ *and* $\ln k_j = \ln P - 10^3(\Delta H_a/R)(1/T)$ *where the pertinent parameters are listed in Table VI,* ΔH_a *is in kcal/mole,* $a_{H^+} = 10^{-pH}$ *and* T *is in degrees Kelvin.*

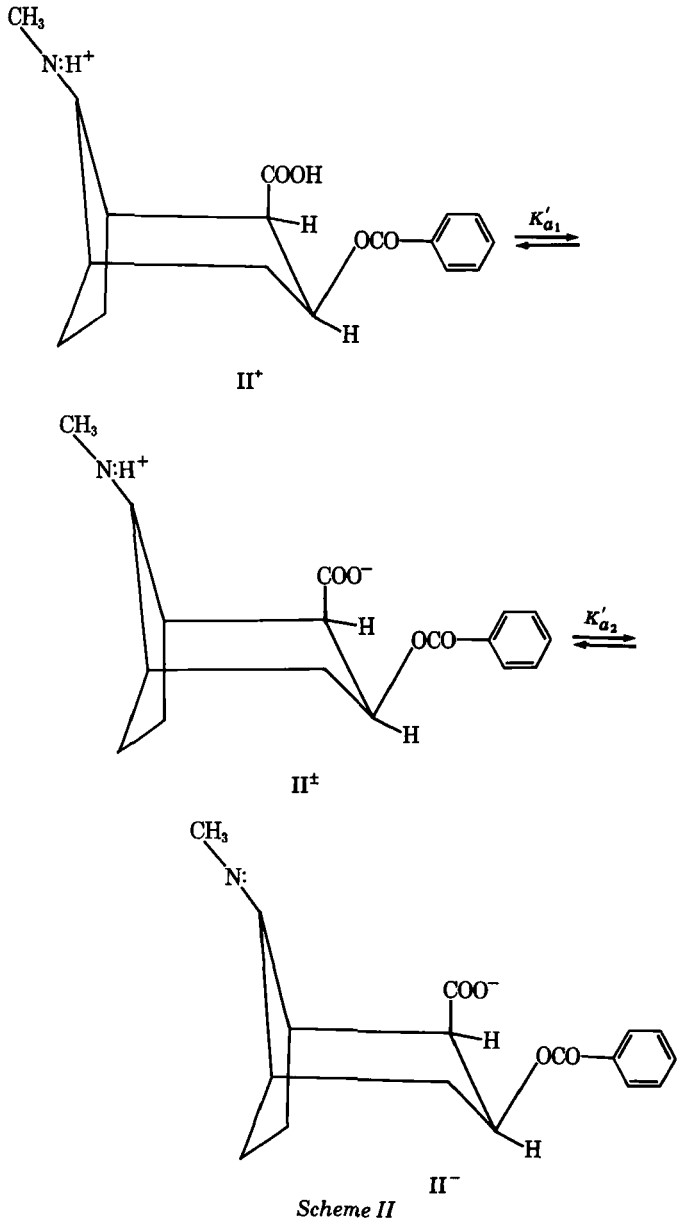

Scheme II

mate temperature dependency, the expression was $1938(1/T) + 2.22$. These values were used in the predicted log k–pH profiles of Figs. 9–11 and are listed in Table VI. The kinetic pK'_a of 7.7 at 80° was estimated from previously reported data (5) on the assumption that the given pH values were measured at the temperature of the reaction. Unfortunately, it was not stated (5) whether or not this was true, so that the possibility of erroneously chosen pH values at 80° cannot be excluded.

The apparent first-order rate constants given previously (5) for studies conducted at 80° and at concentrations tenfold higher than those studied here agreed with the predicted values (Fig. 9) in the 5–6.5 and 0–2 pH ranges. The values were significantly higher than the predicted values in the 2.5–4.5 range. It was probably due to the observed (5) enhancing buffer effects on rate by the citric acid–potassium citrate buffer solution used in the pH 2.2–4.8 range. No general acid–base effects were observed with the buffers used in these present studies.

Log k_2–pH Profiles for II—The log k_2–pH profiles for the solvolysis of II are given in Fig. 12 and were fitted with the estimated parameters given in Table V. The two pK'_a values for II (Scheme II) at room temperature were determined potentiometrically and were 11.75 and 2.1. In this case the acid branch (Eq. 10) of the log k–pH profile would be for the attack of hydrogen ion on the protonated II, whereas below the pK'_{a2} of 11.75, the alkaline branch would be for the hydroxide ion attack on the zwitterion. Above this value, the attack of hydroxide ion would be on the negatively charged compound, and:

$$k_2 = (k'_{OH})_2 f_{II^+} a_{OH} + (k_{OH})_2 f_{II^\pm} a_{OH} \qquad \text{(Eq. 15)}$$

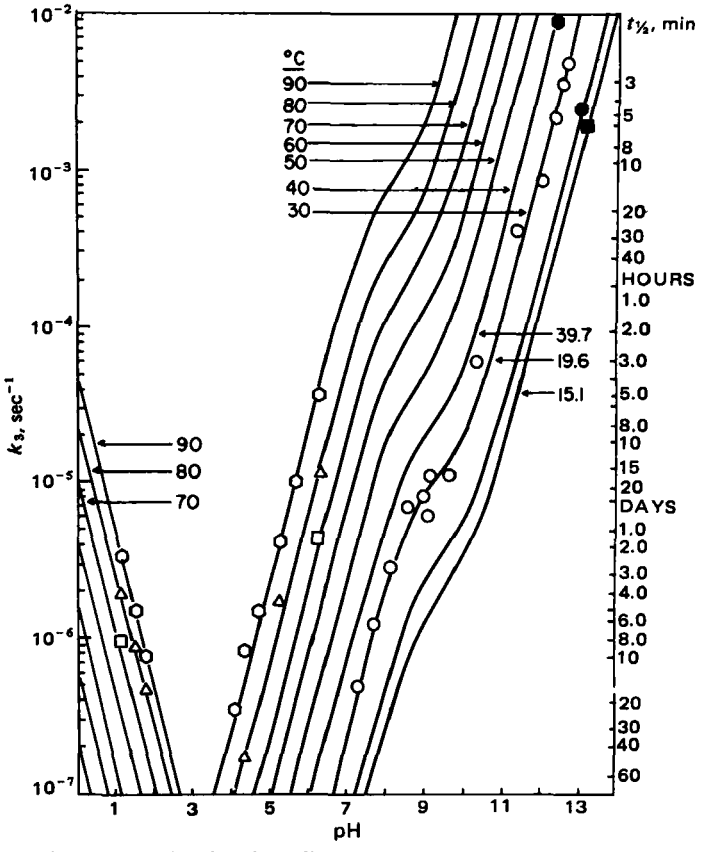

Figure 11—*Fitted and predicted log* k_3*–pH profiles for the hydrolysos of I to IV at the designated temperatures. The fits and predictions are in accordance with:* $k_3 = (k_H)_3 a_{H^+} + (k_{OH})_3 [K_w/(K'_a + a_{H^+})] + (k'_{OH})_3 K'_a K_w/[(K'_a + a_{H^+})a_{H^+}]$ *and ln* $k_j = ln\ P - 10^3(\Delta H_a/R)(1/T)$ *where the pertinent parameters are listed in Table VI,* ΔH_a *is in kcal/mole,* $a_{H^+} = 10^{-pH}$ *and T is in degrees Kelvin.*

where the respective fractions of anionic II (f_{II^-}) and zwitterionic II ($f_{II^\pm}$) >pH 3 are:

$$f_{II^+} = \frac{(K'_{a2})_{II}}{(K'_{a2})_{II} + a_{H^+}} \qquad \text{(Eq. 16)}$$

and:

$$f_{II^\pm} = \frac{a_{H^+}}{(K'_{a2})_{II} + a_{H^+}} \qquad \text{(Eq. 17)}$$

where the pertinent charged structures are given in Scheme II.

Thus, the alkaline branch above pH 6 can be fitted to:

$$k_2 = \frac{(k'_{OH})_2 (K'_{a2})_{II} K_w}{[(K'_{a2})_{II} + a_{H^+}]a_{H^+}} + \frac{(k_{OH})_2 K_w}{(K'_{a2})_{II} + a_{H^+}} \qquad \text{(Eq. 18)}$$

and the acid branch $<pK'_{a1}$ of 2.1 can be fitted to:

$$k_2 = (k_{H^+})_2 f_{II^+} a_{H^+} \qquad \text{(Eq. 19)}$$

where the fraction of protonated II (Scheme II) is:

$$f_{II^+} = \frac{a_{H^+}}{(K'_{a1})_{II} + a_{H^+}} \qquad \text{(Eq. 20)}$$

The fact that there is a pH-independent segment of the log k_2–pH profile at pH 4–5 at the studied temperatures of 80 and 90°, indicates an additional functional dependency for the first-order rate constant, k_2. This additional factor can be rationalized by an hydroxyl ion attack on positively charged II or its kinetic equivalent of water attack on the zwitterion ($II^\pm$):

$$(k_0)_2 f_{II^\pm} = (k''_{OH})_2 a_{OH} f_{II^+} = (k_0)_2 \frac{K'_{a1}}{a_{H^+} + K'_{a1}}$$

$$= (k''_{OH})_2 a_{OH} \frac{a_{H^+}}{a_{H^+} + K'_{a1}} = \frac{(k''_{OH})_2 K_w}{a_{H^+} + K'_{a1}} \qquad \text{(Eq. 21)}$$

where $(k''_{OH})_2 K_w = (k_0)_2 K'_{a1}$.

Thus, an additional dip ~pH 2–4 in the log k_2–pH profile of II can be

Table VI—Parameters for the log k_i^a–pH Profiles for the Hydrolyses of I

Temperature	$10^7 k_H$	k_{OH}	$10^2 k'_{OH}$	$10^7(k_H)_1$	$(k_{OH})_1$	$10^3(k'_{OH})_1$	$10^7(k_H)_3$	$(k_{OH})_3$	$10^2(k'_{OH})_3$	pK'^b_a
15.1	4.0	6.6	2.74	0.75	6.0	0.99	0.82	0.57	2.57	8.94
19.6	6.0	8.8	3.70	1.4	8.4	1.34	1.29	0.78	3.48	8.84
30.0	14.0	18.6	7.65	3.3	17.0	2.33	3.25	1.70	7.76	8.61
39.7	30.0	34.0	15.2	8.0	29.8	4.60	8.00	3.0	14.3	8.41
50.0	64.0	64.0	31.5	18.3	56	7.00	18.0	5.4	28.8	8.22
60.0	130	114	58.5	41.0	98	11.9	40.5	9.5	56.5	8.04
70.0	240	196	100	84.0	160	19.0	83.0	16.0	95.0	7.87
80.0	450	330	170	170	280	29.0	180	26.0	163	7.71
90.0	800	537	290	320	424	45.0	330	54.9	270	7.55
ΔH_a	15.1	12.3	13.0	16.9	11.8	10.6	16.8	11.8	13.1	
ln P	11.52	23.30	19.14	13.05	22.47	11.64	13.03	20.05	19.17	
$\Delta S^\ddagger$	−35.8	−12.3	−20.6	−32.7	−14.0	−35.5	−32.7	−18.8	−20.5	

[a] Log k_i–pH profiles are from Figs. 9–11; the apparent first-order rate constants (k, k_1, and k_3) for the routes of Scheme I are in sec^{-1}, where the given bimolecular rate constants are in liter/mole/sec, ΔH_a is in kcal/mole, and $\Delta S^\ddagger$ is in entropy units (eu) where $\Delta S^\ddagger = R[\ln P - (\ln k_B T/k)]$, the Boltzmann constant $k_B = 1.387 \times 10^{-16}$ erg/deg and the Planck constants $h = 6.623 \times 10^{-27}$ erg sec, and T is 313°K. [b] Values at 30 and 80° were obtained from the best log k–pH fit at these temperatures. Values at other temperatures were calculated from $pK'_a = 1938(1/T) + 2.22$.

predicted (dashed line in Fig. 12). This could be calculated exactly if the K'_{a1} values of Eq. 20 were known at all temperatures. The total dependency would be:

$$k_2 = (k_H)_2 a_{H^+} \frac{a_{H^+}}{a_{H^+} + K'_{a1}} + (k_0)_2 \frac{K'_{a1}}{a_{H^+} + K'_{a1}} + (k_{OH})_2 \frac{K_w}{K'_{a2} + a_{H^+}} + (k'_{OH})_2 \frac{K'_{a2} K_w}{[K'_{a2} + a_{H^+}] a_{H^+}} = (k_H)_2 a_{H^+} f_{II^+} + [(k_0)_2 + (k_{OH})] f_{II^\pm} + (k'_{OH})_2 f_{II^-} \quad \text{(Eq. 22)}$$

Temperature Dependency and Strategy for Stability Prediction—Studies of this nature delineate stabilities or reaction rates at all temperatures and pH-values with a minimum of experimental effort. An appropriate strategy is to determine first the functional kinetic dependencies from the dependence of the apparent first-order rate constant, k, on pH at a given temperature. If this were accomplished, pH regions could be ascertained where the only significant reaction was due to the attack of one ion on only one ionic species of substrate, *e.g.*, hydroxyl ion attack on protonated I with a bimolecular rate constant of k_{OH}. Similarly, the k_H bimolecular rate constant (Eq. 22) for hydrogen ion catalysis could be determined in the highly acidic pH region.

The specific bimolecular rate constant for hydroxyl ion catalysis, k_{OH}, of a unique ionic substrate species can be determined readily, since:

$$\log k_{OH} = \log k + pK_w - \text{pH} \quad \text{(Eq. 23)}$$

and k_{OH} can be estimated from any k–pH pair in the region where a linear positive slope of unity exists in the log k–pH profile. Similarly, the bimolecular rate constant for hydrogen ion catalysis, k_H, of a unique ionic substrate species can be determined from:

$$\log k_H = \log k + \text{pH} \quad \text{(Eq. 24)}$$

and k_H can be estimated from any k–pH pair where a linear negative slope of unity exists in the log k–pH profile.

Such bimolecular rate constants, k_j, which may be either k_{OH}, k'_{OH}, or k_H, can be related to temperature by the Arrhenius rule:

$$\ln k_j = \ln P - \left(\frac{10^3 \Delta H_a}{R}\right)\frac{1}{T} \quad \text{(Eq. 25)}$$

where ΔH_a is the heat of activation (kcal/mole) and T is the absolute temperature (degrees Kelvin). The k_j-values at several temperatures could be estimated from a single k–pH pair obtained at a given temperature in the pH region, where only one catalytic process was extant. Arrhenius plots of such bimolecular rate constants for the solvolysis of I and II in accordance with Eq. 25 are given in Fig. 13, and the determined Arrhenius parameters, ΔH_a and ln P, are listed in Tables VI and VII. For the experimental convenience of limiting the times of kinetic studies without being excessively fast, Arrhenius parameters were obtained at high temperatures (70–90°) for hydrogen ion (k_H) and hydroxyl ion (k_{OH}) attack on protonated I ($I{\cdot}H^+$) and at low temperatures (15–40°) for hydroxyl ion attack (k'_{OH}) on neutral I (Figs. 9–11). Similar choices of appropriate temperatures and pH ranges were made in the studies of II (Fig. 12) for appropriate calculations of bimolecular rate constants (k_j) and subsequent estimations of their Arrhenius parameters (Fig. 13, Table VII).

If pK'_a values were known at several temperatures, as from independent potentiometric titrations, the apparent first-order rate constants, k_i, could be calculated readily in the intermediate pH regions where several rate processes exist concomitantly, from expressions such as Eq. 14 for the solvolysis of I and Eqs. 18 and 22 for the solvolysis of II. The respective bimolecular rate constants, k_j, at the respective temperatures as listed in Tables VI and VII could be calculated from Eq. 25 using the determined Arrhenius parameters.

If apparent first-order rate constants were obtained in the pH region of transition from one rate process to another (*e.g.*, at pH 7–11 where solvolytic dependencies of I change from hydroxyl ion attack on the protonated species to that on a neutral species as in Figs. 9–11), the pK'_a for the dissociation of the substrate as an acid can be obtained by fitting the more complex dependency of the apparent first-order rate constant, k, on pH on K'_a. In the case of I, Eq. 14 was fitted with a best-estimated pK'_a in this transition region at 30°, where k_{OH} and k'_{OH} had been determined from linear segments of the log k–pH profiles from application of Eq. 23.

In the case of II, Eq. 18 could be fitted with a best-estimated K'_{a2} in the transition pH region where reaction dependency changes from hydroxyl ion attack on the zwitterion to hydroxyl ion attack on the anion of II if the $(k_{OH})_2$ and $(k'_{OH})_2$ values were known. Unfortunately, the high pK'_{a2} (11.75 at room temperature) of the zwitterion of II (Scheme III) does not

Table VII—Parameters for the log k_2^a–pH Profiles for the Hydrolyses of II

Temperature	$10^7(k_H)_2$	$10^9(k_0)_2^a$	$10^2(k_{OH})_2$	$10^3(k'_{OH})_2$	pK'_{a2}	pK_w
15.1	0.68	0.93	2.4	5.53	12.5	14.30
19.6	1.11	1.50	3.4	7.98	12.2	14.15
30.0	3.52	4.60	7.4	12.5	11.7	13.83
39.7	9.50	13.0	15.2	34.7	11.3	13.56
50.0	26.0	32.0	29.5	112	10.8	13.28
60.0	67.0	80.3	57.0	253	10.3	13.03
70.0	150	180	100	410	9.9	12.79
80.0	350	400	202	750	9.6	12.57
90.0	700	800	241	1300	9.2	12.35
ΔH_a	19.4	18.9	13.8	15.2		
ln P	17.39	12.26	20.30	21.34		
$\Delta S^\ddagger$	−24.1	−34.3	−18.3	−16.2		

[a] The log k_2 profiles are from Fig. 12; the given bimolecular rate constants are in liter/mole/sec, ΔH_a is in kcal/mole, $\Delta S^\ddagger$ is in entropy units (eu) where $\Delta S^\ddagger = R[\ln P - (\ln k_B T/k)]$ and the Boltzmann constant $k_B = 1.387 \times 10^{-16}$ erg/deg, and the Planck constant $h = 6.623 \times 10^{-27}$ erg/sec, and T is 313°K. The apparent first-order rate constants k_2 and k_0 are in sec^{-1}.

Table VIII—Arrhenius Parameters [a] for Apparent First-Order Rate Constants for Solvolysis of I Under Different Conditions

Medium	pH	k		k_1		k_2		k_3	
		ΔH_a	$\ln P$	ΔH_a	$\ln P$	ΔH_a	$\ln P$	ΔH_a	$\ln P$
0.1 *M* HCl	1.11	15.9	10.00	16.5	9.97	17.2	11.65	14.6	7.68
Phosphate buffer	6.25	26.2	11.15	26.5	28.8	13.9	6.31	27.3	27.62
0.0884 *M* NaOH	12.17	11.2	13.31	11.6	11.2	8.76	8.17	11.4	13.55

[a] The parameter $\ln k_i = \ln P - (10^3\,\Delta H_a/R)(1/T)$ where R = 1.987 cal/deg and ΔH_a is in kcal/mole.

permit the immediate determination of $(k'_{OH})_2$ from a linear segment of the pH profile (Fig. 12) above a pH equal to pK'_{a2}. The experimentally determined apparent first-order rate constants (k_2) for the solvolysis of II in strong alkali were still in the region of the pK'_{a2} value. Estimates of both pK'_{a2} and $(k'_{OH})_2$ that were consistent with the first-order rate constants, k_2 in this transition region, were made in accordance with Eq. 18 and are given in Table VII. These pK'_{a2} values can be characterized by $4556(1/T) - 3.33$. The pK'_{a2} values calculated accordingly were used in the predicted log k_2–pH profiles of Fig. 12 and are listed in Table VII.

There is a caveat for those who wish to use these strategies in prediction of stabilities. Prediction at temperatures other than those studied should not be made based on Arrhenius parameters (Eq. 25, Table VIII, Fig. 14) for studies conducted in the same buffer solutions at several temperatures. Comparison of apparent heats of activation for the bimolecular rate constants (Table VI) and the apparent first-order rate constants (Table VIII) shows wide discrepancies in many instances. For example, the estimated $(\Delta H_a)_{k_j}$ (kcal/mole) for the apparent first-order rate constants of solvolysis of I in pH 6.25 phosphate buffer were 26.2, k; 26.5, k_1; and 27.3, k_3; whereas the $(\Delta H_a)_{k_j}$ values for the bimolecular rate constants representative of hydroxyl ion attack on protonated I were 12.3, k_{OH}; 11.8, $(k_{OH})_1$; and 11.8, $(k_{OH})_3$. These latter values are typical of hydroxyl ion-catalyzed solvolysis of esters.

The reason for these discrepancies are simple. Since:

$$k = k_{OH}a_{OH} = k_{OH}K_w/a_{H^+} \qquad \text{(Eq. 26)}$$

or in general:

$$k_i = k_j a_{OH} = k_j K_w/a_{H^+}$$

then:

$$\ln k = \ln k_{OH} - \text{pOH} = \ln k_{OH} + \text{pH} - pK_w \qquad \text{(Eq. 27)}$$

Each apparent logarithm of the rate constant and that of the K_w can be expressed by a relation such as Eq. 25, and therefore:

$$\ln P_{k_i} - (\Delta H_a)_{k_i}/RT = \ln P_{k_j} - (\Delta H_a)_{k_j}/RT + \text{pH} - (\ln P_{K_w} + \Delta E_{K_w}/RT) = \ln P_{k_j} - \ln P_{K_w} + \text{pH} - [(\Delta H_a)_{k_j} - (\Delta E)_{K_w}]/RT \qquad \text{(Eq. 28)}$$

Table IX—Red Blood Cell Partitioning of I

	$[I]_0$, μg/ml	Equilibration time, min	D
Whole blood	10	60	0.754
	10	120	0.752
Red blood cell–phosphate buffer (pH 7.4)	10	60	0.789
	10	120	0.612
Red blood cell–plasma water	4	35	0.758
	3	35	0.902
	2	35	0.753

Table X—Red Blood Cell Partitioning of II [a]

		D	
$[II]_0$	Blood	Red Blood Cell–Phosphate Buffer (pH 7.4)	Red Blood Cell–Plasma Water
10	0.91	0.88	—
5	1.18	1.34	1.34
1	0.88	0.66	0.95, 0.84
0.5	0.85	0.98	—
2.5	0.88, 0.67, 0.74	—	—

[a] After 25-min equilibration.

Thus:

$$\ln P_{k_i} = \ln P_{k_j} - \ln P_{K_w} + \text{pH} \qquad \text{(Eq. 29)}$$

and entropies of activation calculated from $\ln P_{k_i}$ are pH dependent and are not valid estimates. Also:

$$(\Delta H_a)_{k_i} = (\Delta H_a)_{k_j} - \Delta E_{K_w} \qquad \text{(Eq. 30)}$$

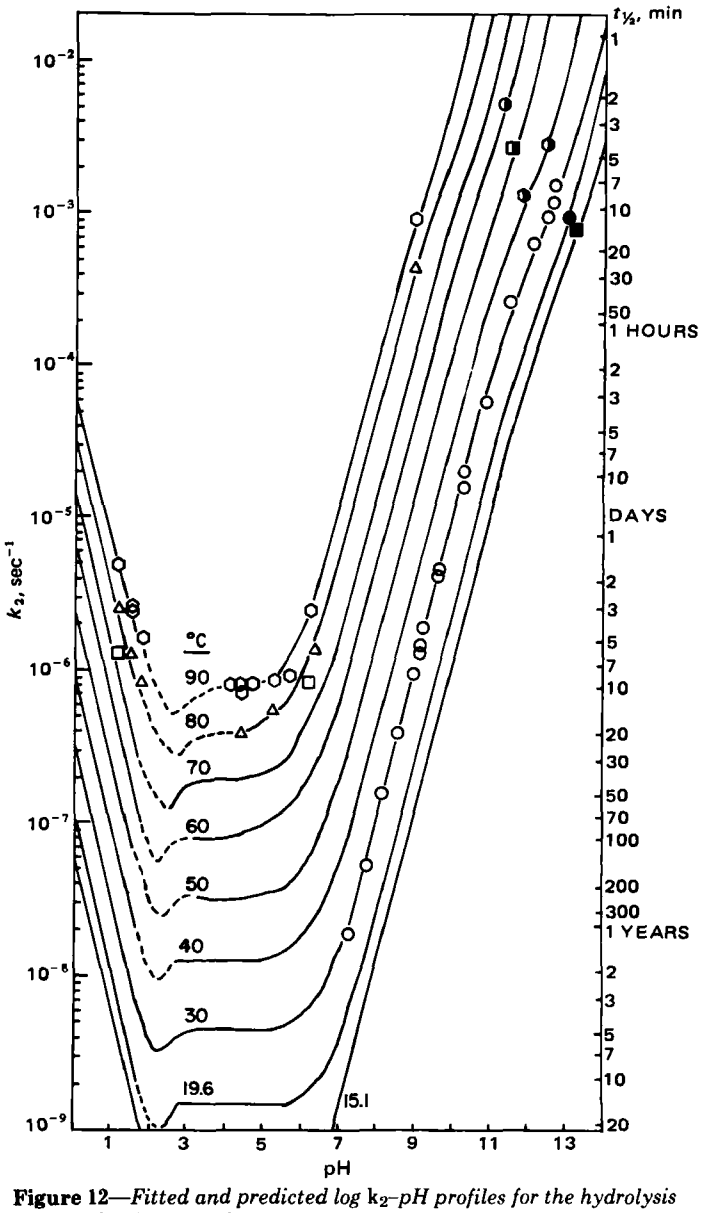

Figure 12—*Fitted and predicted log* k_2*–pH profiles for the hydrolysis of II at the designated temperatures. The fits and predictions are in accordance with:* $k_2 = (k_H)_2 a_{H^+}\,[a_{H^+}/(a_{H^+} + K'_{a_2})] + (k_0)_2\,[(K'_a)_1/(a_{H^+} + K'_{a_1})] + (k_{OH})_2\,[K_w/(K'_{a2} + a_{H^+})] + (k'_{OH})_2\,[K'_{a2}K_w/(K'_{a2} + a_{H^+}a_{H^+})]$ *and* $\ln k_j = \ln P - 10^3(\Delta H_a/R)(1/T)$ *where the pertinent parameters are listed in Table VII,* ΔH_a *is in kcal/mole,* $a_{H^+} = 10^{-pH}$ *and T is in degrees Kelvin. Since the* $p(K'_a)_1 = 2.1$ *was only estimated at room temperature, the given dashed segments of the profiles at other temperatures are only estimates of the dependencies.*

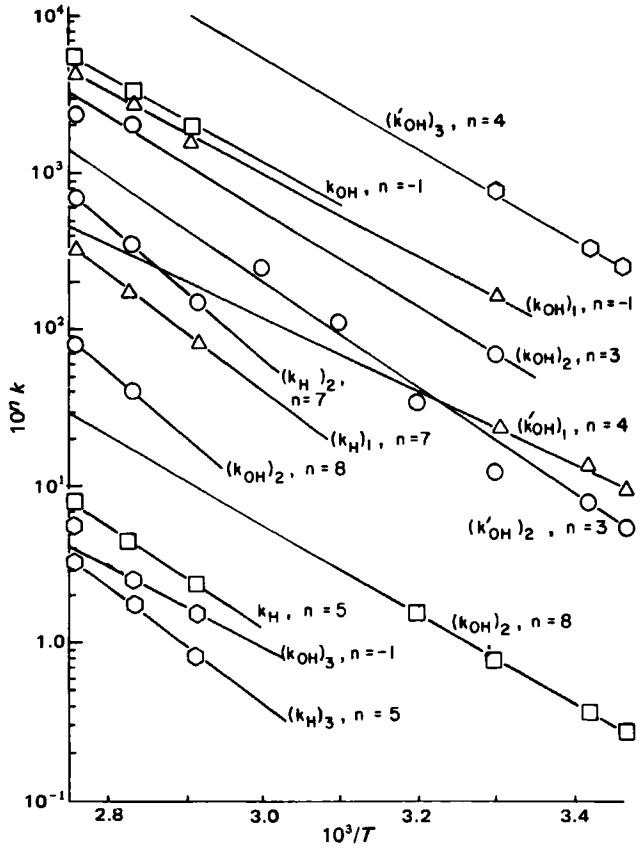

Figure 13—*Arrhenius plots (ln* k_j, *liters mole*$^{-1}$ *sec*$^{-1}$, versus *1/T where T is in degrees Kelvin) for the bimolecular rate constants for hydrogen ion-catalyzed solvolyses of I: overall,* k_H; *to II* $(k_H)_1$; *to IV* $(k_H)_3$; *and for the acid-catalyzed solvolysis of II,* $(k_H)_2$. *Also, for the hydroxyl ion-catalyzed solvolysis of protonated and neutral I, respectively: overall,* k_{OH} *and* k'_{OH}; *to II,* $(k_{OH})_1$ *and* $(k'_{OH})_1$; *to IV,* $(k_{OH})_3$ *and* $(k'_{OH})_3$; *and for the respective hydroxyl ion-catalyzed solvolysis of zwitterionic and anionic II,* $(k_{OH})_2$ *and* $(k'_{OH})_2$. *The* $(k_0)_2$ *is for the attack of water on the zwitterion of II.*

and heats of activation calculated from the apparent first-order rate constants obtained from the same buffer solutions studied at different temperatures always exceed the heats of activation calculated from the bimolecular rate constants and are not valid estimates.

The assertions (5) that the maximum stability of I was pH 1.95 and that II was the solvolytic product needs to be modified in light of these present studies; compound IV is also produced (Tables III and IV, Fig. 11). The maximum stabilities of I are at the minima of the log-pH profiles of Fig. 9 and vary between pH 3.2 and 3.8 from 15 to 90°. The maximum stabilities of II (Fig. 12) are ~pH 1.8.

The apparent heats of activation of the apparent first-order rate constants for solvolysis of I were given previously (5) as 22.9 kcal/mole at pH 6.8, 25.6 kcal/mole at pH 5.0, and 23.4 kcal/mole at pH 2.2. The values were not inconsistent with that of 26.2 kcal/mole determined at pH 6.25 in this investigation.

Applications of Plasma Assays to Stabilities of I in Fresh Plasma—The stability of I was monitored by HPLC assay in fresh dog plasma. A study of 8.8×10^{-3} *M* (299 μg/ml) I at 38.9° (Fig. 15) by HPLC Procedure II showed an apparent half-life of 5.44 hr ($k = 3.54 \times 10^{-5}$ sec^{-1}), close to the half-life of I in phosphate buffer at that temperature (Table IV, Fig. 9). The data for II in Fig. 15 could be well-fitted by the procedures outlined relative to Eqs. 4–8 and were consistent with 90% of I being hydrolyzed through the route for hydrolysis of II, the same product of aqueous solvolysis at this pH. An approximate estimate of hydrolysis of II could be estimated with a half-life of >100 hr ($k_2 = 1.9 \times 10^{-6}$ sec^{-1}).

An additional study at an initial concentration of 8.8×10^{-4} *M* I in dog plasma (30 μg/ml) using HPLC procedure III showed a similar apparent half-life (Fig. 15) for I of $t_{1/2}$ = 6.0 hr and demonstrated no significant change for this tenfold dilution of substrate. However, the fraction hydrolyzing through the route for II was only 0.5 under these conditions.

Additional studies on plasma stability of I were conducted at 1000, 500, and 250 ng/ml in the same fresh dog plasma by HPLC procedure IV (Fig. 15) and showed half-lives of 1.98, 2.08, and 1.9 hr, respectively. This signified a more than doubling of the plasmolysis rate at the lower concentrations of I to indicate a possible saturation of hydrolyzing enzymes at the higher concentrations of I. The possible increase in hydrolysis rates (dashed lines, Fig. 15) at high initial cocaine concentrations was confirmed.

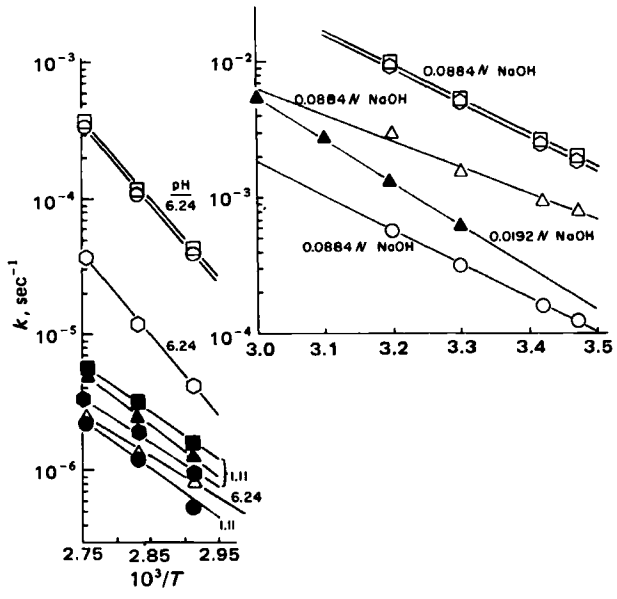

Figure 14—*Arrhenius plots (ln* k_i *sec*$^{-1}$ versus *1/T where T is in degrees Kelvin) for (□)* k, *(○)* k_1, *(△)* k_2, *and* k_3 *(○) rate constants at the labeled specified conditions.*

Red Blood Cell–Plasma and –Buffer and –Plasma Water Partitioning and Protein Binding of I and II—The assayed plasma or plasma water concentrations of I, $[I]_p$, were substituted into the following

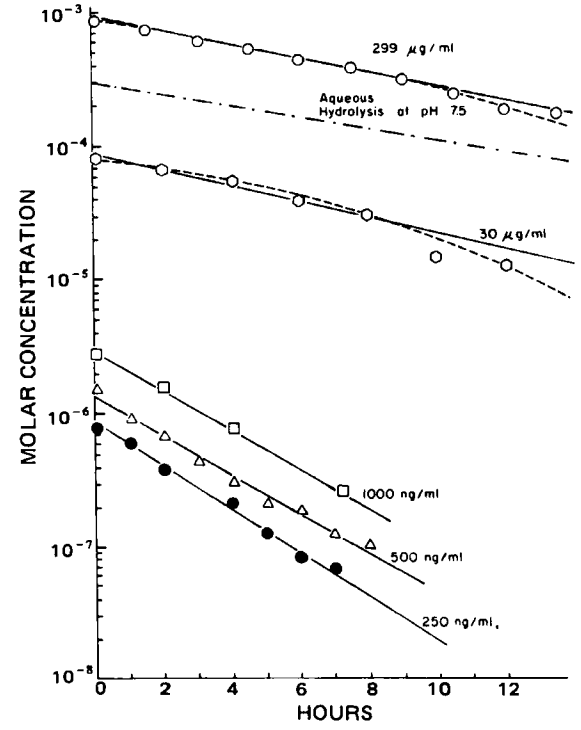

Figure 15—*Semilogarithmic plots of I in fresh dog plasma against time at 38.9° with the designated initial concentrations of I* (I_0). *The solid lines were drawn on the premise of first-order disappearance of I, although accelerating rates with time (dashed lines) are possible at the higher concentrations. The time course of hydrolysis of I in aqueous pH 7.5 buffers is also given (---) for comparison. Key: (●) 250 ng/ml; (△) 500 ng/ml; (□) 1000 ng/ml; (○) 30 μg/ml; (○) 299 μg/ml.*

equation to determine the concentration of I in red blood cells ($[I]_{RBC}$):

$$[I]_{RBC} = \frac{I - [I]_p V(1 - H)}{VH} \quad \text{(Eq. 31)}$$

where I is the amount of cocaine added to a volume (V) of blood or synthetic blood with an H fraction of this volume as red blood cells. The I-values used were calculated from $I = I_0 e^{-kt}$ where I_0 is the amount of I added at t minutes before assay, and k is the apparent first-order rate constant of degradation of I in the system. The apparent red blood cell–plasma partition coefficient was $D = [I]_{RBC}/[I]_p$; values are given in Table IX. The fact that there is no significant difference among systems with and without plasma proteins is indicative of no significant protein binding of I.

Similar studies were conducted with II (Table X). Although the data are more variable than in the case for I, the reasonable consistency of red blood cell–plasma and red blood cell–buffer or plasma water coefficients (D) in parallel studies at a given concentration of II ($[II]_0$) is indicative of negligible plasma protein binding of II.

Since I has relatively high solvolysis rates in plasma and buffers, plasma protein binding studies by equilibrium dialysis or ultracentrifugation are not applicable, since they take relatively long periods of time. An attempt to use ultrafiltration through filter cones (17) was not satisfactory, since I was variable and highly bound to the filter cones. When 4 ml of plasma and 4 ml of plasma–water were filtered to the same extent through individual fresh cones, the percent of the filtered 1-μg/ml solution recovered was 32 ± 1% for plasma–water and 23 ± 1% for plasma to indicate a possible plasma protein binding of 8% for I. The filter cones were pre-equilibrated with buffer containing the same concentrations of I in plasma that were to be filtered through those same cones. The percent concentration recovered in the filtrate in the same cone from buffer filtration and subsequent plasma filtration, respectively, was 46.3 and 54.6 at 2 μg/ml and 48.8 and 54.6 at 1 μg/ml.

However, when the same two filtrations in the same cone were effected using only buffer, the percent concentration of I recovered in the same cone was 43.8 and 56.2 at 1 μg/ml and 38.8 and 61.3 at 0.5 μg/ml. This mimicked the situation when the second filtration was of I-spiked plasma to show that the loss of I in the filtrate was due to its binding to the cones on successive filtrations and that it could not be assigned to plasma protein binding.

REFERENCES

(1) R. L. Foltz, A. F. Fentiman, and R. B. Foltz, NIDA Research Monograph 32, Aug. 1980, pp. 90–109.

(2) P. I. Jatlow and D. N. Bailey, *Clin. Chem.*, **21**, 1918 (1975).

(3) G. Barnett, R. Hawks, and R. Resnick, *J. Ethnopharmacol.*, **3**, 353 (1981).

(4) J. I. Javaid, H. Dekirmenjian, J. M. Davis, and C. R. Schuster, *J. Chromatogr.*, **152**, 105 (1978).

(5) J. B. Murray and H. I. Al-Shora, *J. Clin. Pharmacy*, **3**, 1 (1978).

(6) E. R. Garrett, in "Advances in Pharmaceutical Sciences" vol. II, H. S. Bean, A. H. Beckett, and J. E. Carless, Eds., Academic, New York, N.Y., 1967, pp. 1–94.

(7) E. R. Garrett, *J. Pharm. Educ.*, **44**, 347 (1980).

(8) E. R. Garrett and R. Barbhaiya, *J. Pharm. Sci.*, **70**, 39 (1981).

(9) E. R. Garrett and M. R. Gardner, *ibid.*, **71**, 14 (1982).

(10) P. I. Jatlow, C. Van Dyke, P. Barash, and R. Byck, *J. Chromatogr.*, **152**, 115 (1978).

(11) M. A. Evans and T. Morarity, *J. Anal. Toxicol.*, **4**, 19 (1980).

(12) J. E. Lindgren, *J. Ethnopharmacol.*, **3**, 337 (1981).

(13) T. V. Parke and W. W. Davis, *Anal. Chem.*, **26**, 642 (1954).

(14) Stat-1-22A "Linear Regression" HP-65 Stat Pac I, Hewlett-Packard, Cupertino, Calif., pp. 49–51.

(15) H. S. Harned and B. B. Owen, "The Physical Chemistry of Electrolytic Solutions," 3rd ed. Reinhold, New York, N.Y., 1958.

(16) S. Glasstone, "Textbook of Physical Chemistry," 2nd ed., D. Van Nostrand, New York, N.Y., 1946, p. 1075.

(17) P. H. Hinderling, J. Bres, and E. R. Garrett, *J. Pharm. Sci.*, **63**, 1684 (1974).

ACKNOWLEDGMENTS

Supported in part by Grant 2-R01-DA-00743 from the National Institute of Drug Abuse, Rockville, MD 20852.

Spectral Analysis of the Configuration and Solution Conformation of Dihydrodigoxigenin Epimers

HOWARD N. BOCKBRADER * and RICHARD H. REUNING ˣ

Received November 21, 1980, from the *College of Pharmacy, The Ohio State University, Columbus, OH 43210.* Accepted for publication May 12, 1982.

*Present address: Pharmaceutical Research Division, Warner-Lambert/Parke-Davis, Ann Arbor, MI 48106.

Abstract □ The C_{20} configuration and solution conformation of each epimer of dihydrodigoxigenin has been studied by circular dichroism (CD) and NMR spectroscopy. Results from the CD spectra indicate that the two epimers have opposite orientations of the β-carbon in the lactone ring. This finding, together with X-ray crystallographic data from a separate study on the minor epimer, establishes the C_{20} configuration of the minor epimer as *S* and of the major epimer as *R*. NMR evidence indicates that the average lactone rotamer for the minor epimer has the C_{22} position located on the C_{12} side of the steroid nucleus, whereas the average lactone rotamer for the major epimer has the C_{21} position located on the C_{12} side of the steroid nucleus. Molecular models indicate that these are the least-hindered positions for the respective rotamers. Physical data characterizing the two epimers are provided.

Keyphrases □ Dihydrodigoxigenin—epimers, spectral analysis of the configuration and solution conformation □ Spectral analysis—configuration and solution conformation of dihydrodigoxigenin epimers □ Epimers, dihydrodigoxigenin—spectral analysis of the configuration and solution conformation

Since the discovery of dihydrodigoxigenin (I) in the urine of a patient requiring large doses of digoxin (1) and the discovery of the metabolite dihydrodigoxin (II) in the plasma samples of three different subjects (2), a significant amount of research has been carried out on the digoxin cardanolide metabolites that are reduced at the C_{20}—C_{22} bond. Previous studies (3, 4) found 0.2–2% of the total radioactivity in urine as II in seven subjects after an oral dose of tritiated digoxin. Excretion of 12–20% of the digoxin maintenance dose as II in the urine of nine patients has also been reported (5, 6). Others (7) have found an average of 13% (range 1–47%) of the total glycosides in the meth-

0022-3549/83/0300-0271$01.00/0